Part 2—Glaciological Topics

Tidewater Glaciers

Of the tens of thousands of glaciers in Alaska, only about 0.1 percent end in the ocean, in the glacial-marine environment (Molnia, 1983a). These glaciers are known as tidewater glaciers, a term introduced by Russell (1893) and defined as "glaciers which enter the ocean and calve off to form bergs." A similar definition, a "glacier that terminates in the sea, where it usually ends in an ice cliff from which icebergs are discharged," is given in the *Glossary of Geology* (Jackson, 1997, p. 665). According to Mark F. Meier (written commun., 2004) all of Alaska's tidewater glaciers are grounded at their beds (a criterion included in the Meier and Post, 1987, definition of a tidewater glacier). Meier also noted that tidewater glaciers are not to be confused with "floating glaciers," such as ice tongues and ice shelves. A discussion of "ice walls" (grounded glacier ice) and "ice fronts" (floating glacier ice) is given by Swithinbank (1988, p. B4, *http://pubs.usgs.gov/prof/p1386b/*). Today the ocean-terminating tidewater glaciers are termed marine tidewater glaciers to distinguish them from an even larger group of lacustrine-terminating calving glaciers.

Calving is defined as the "breaking away of a mass or block of ice from a glacier" (Jackson, 1997, p. 92). In tidewater glaciers, the rate of calving controls the glacier's length much more than climate. "Calving glaciers" lose most of their mass by calving rather than by surface melting. Typically, the terminus of a marine tidewater calving glacier has a steep, near-vertical to vertical face characterized by significant fracturing and the presence of seracs (fig. 39). Rapid calving often produces amphitheater-shaped embayments, some many hundreds of meters in diameter in the face (fig. 40). In some glaciers, the rate of calving and the volume of ice calved are so great, that no open water can be seen in front of the glacier margin.

Figure 39.—*15 July 1979 photograph of the 60-m-high terminus of Muir Glacier, St. Elias Mountains, which was a calving tidewater glacier at that time. The steep vertical face characterized by significant fracturing and the presence of seracs is typical of tidewater calving glaciers. Photograph by Bruce F. Molnia, U.S. Geological Survey.*

Tidewater glaciers can exhibit rapid changes in terms of the speed of advance and retreat of their termini and the flow of glacier ice. Hubbard Glacier, which retreated through much of the "Little Ice Age," has been advancing for more than 100 years. Molnia and Post (1995) reported that, between 1967 and 1993, Bering Glacier had retreated as much as 10.7 km (an average of approximately 450 m a^{-1}, with a maximum retreat of 2,600 m between 1977 and 1978).

From a detailed analysis of topographic maps and aerial photography, Viens (1995) determined that there were 51 Alaskan tidewater glaciers and 9 former tidewater glaciers (fig. 41). Some of the tidewater glaciers, like the Columbia Glacier, produce large quantities of icebergs. Some, like Muir Glacier, no longer make contact with the sea at present. The 60 present and former tidewater glaciers have a combined area of about 27,000 km^2, approximately 36 percent of the glacierized area of Alaska. Table 2 is a compilation of information presented by Viens (1995) on the length, total area, accumulation area, ablation area, and accumulation area ratio (the accumulation area divided by the total area of the glacier at the end of the balance year or AAR) of each of the 60 tidewater glaciers that he characterized. Even though some tidewater glaciers may have AARs (see tables 2 and 3) of greater than 0.93, they still are retreating because of calving. Details about the behavior of individual tidewater glaciers will be described by geographic region in the sections that follow.

Figure 40.—*Oblique aerial photograph of the central terminus of Bering Glacier in Vitus Lake, Chugach Mountains, on 16 August 1998. The amphitheater-shaped embayment produced by the rapid calving retreat of the terminus is about 2 km in diameter. Photograph by Bruce F. Molnia, U.S. Geological Survey.*

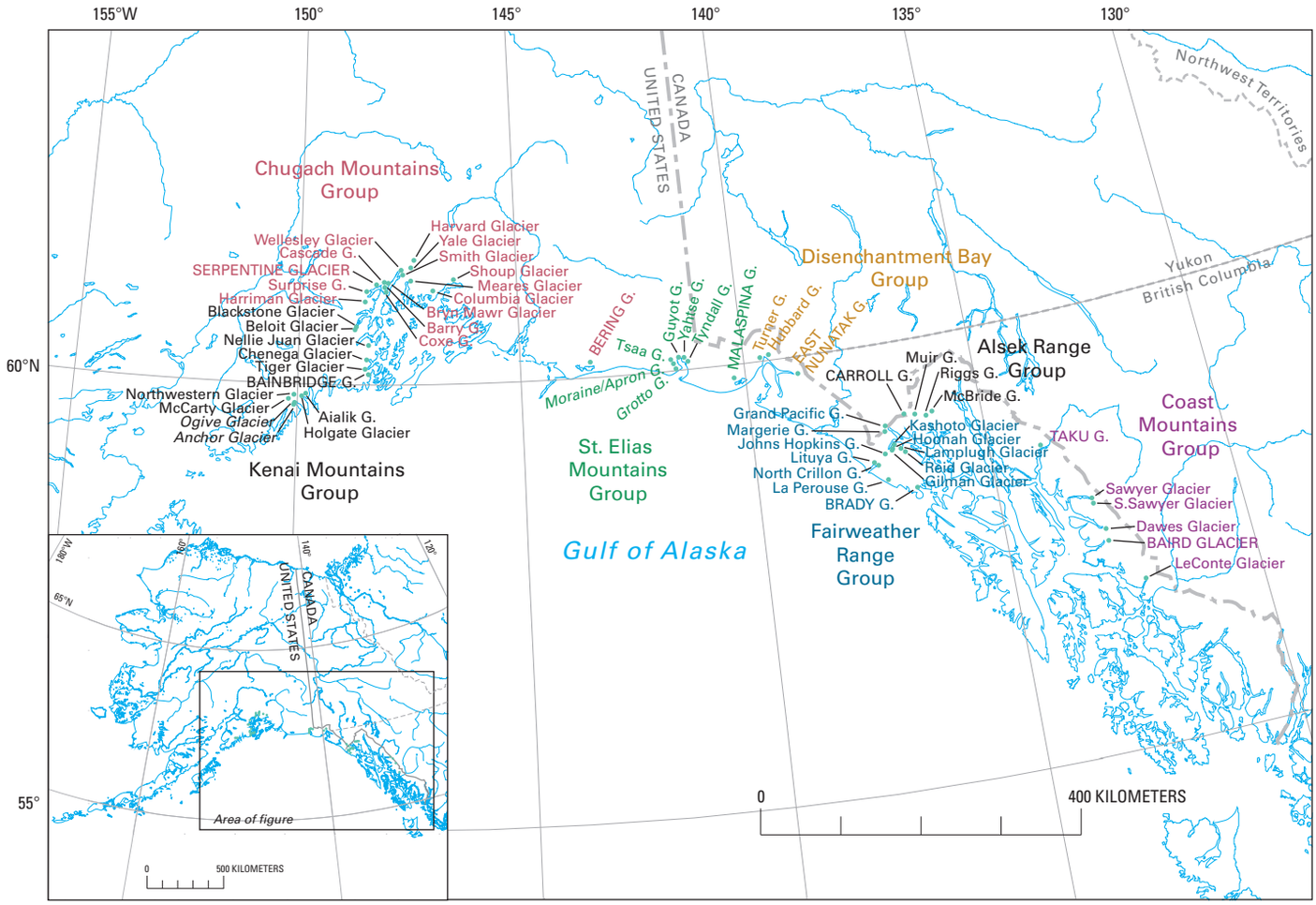

Figure 41.—*Map of active and former tidewater glaciers of Alaska compiled by the editors using glaciers selected by Viens (1995). G indicates glacier. Glacier names in italics have not been approved by the U.S. Board on Geographic Names. Glaciers shown in capital letters were previously classified as tidewater glaciers (tables 2, 3).*

Columbia and Hubbard Tidewater Glaciers

By ROBERT M. KRIMMEL[6]

Introduction

Glaciers that flow into the ocean are known as tidewater glaciers. Figure 41 shows the active and former tidewater glaciers found in Alaska, according to Viens (1995) and Krimmel (tables 2, 3). Some tidewater glaciers, including Columbia Glacier, produce large numbers of icebergs by calving; others barely reach the sea. In Alaska, all tidewater glaciers are grounded on their beds. Loss of mass by calving may exceed the loss of mass by melting by several orders of magnitude in some of the larger and more active tidewater glaciers. Nearly all tidewater glaciers in Alaska have undergone large-scale asynchronous advance and retreat (fig. 42*A*–*D*). Apparently, this behavior is not related directly to climatic variations.

The primary influence on the stability of tidewater glaciers was first suggested by Post (1975) as the water depth at the calving face; calving speed is related directly to water depth—slow in shallow water and faster in deep water. According to Mark F. Meier (written commun., 2004), the validity of this relatively simple concept has been questioned by Van der Veen (1996, 1997b) who suggests that the relationship is more complex. Advancing tidewater glaciers end on a terminal-moraine shoal consisting of unconsolidated material that nearly fills the fjord at the glacier front. Measured water depths near the calving faces of stable and advancing glaciers have been found to be generally less than about 80 m, in comparison with several hundred meters of water in the fjord beyond the shoal (Brown and others, 1982).

On a time scale of hundreds of years, tidewater glaciers advance by moving their submarine terminal moraines down the fjord (fig. 42*B*). The moraine is not simply pushed. The moraine is advanced by glacial erosion of material on the upstream side and redeposition on the downstream side. The deposition produces a series of foreset beds. Foreset bedding has been observed by subbottom sounder profiling (Meier and others, 1978), which supports this theory of moraine advance. The rate of advance of the terminal moraine is slow (rarely more than a few tens of meters per year) in deep fjords and is controlled by the amount of morainal material that must be moved to maintain relatively shallow water at the calving face. An advance generally continues until the glacier becomes increasingly sensitive to external influences, including climate variations, that may cause it to retreat from its moraine shoal (fig. 42*C*).

Drastic retreat of a tidewater glacier normally begins when a small recession from the shoal causes its terminus to recede into deeper water behind the crest of the terminal moraine (fig. 42*D*) (Meier and Post, 1987). Because calving speed may be directly related to the water depth at the terminus (Brown and others, 1982), a retreat into deeper water stimulates an increase in calving speed. Instability develops when the calving speed becomes greater than the ice speed and the retreating calving front moves into even deeper water. Drastic retreat ends when the terminus recedes into shallow water, normally at the head of the fjord (fig. 42*A*). The rate of retreat can be a kilometer or more per year—many times faster than the rate of advance. In most cases, as tidewater glaciers drastically retreat, the AAR increases as the ice in the ablation area is discharged as icebergs. Thus, tidewater glaciers ending near the heads of fjords frequently have high AAR's, whether they are advancing or retreating. Readvance, following a drastic retreat, begins when there is enough morainal material at the calving face to maintain a terminal moraine shoal as the calving face advances into the fjord (fig. 42*B*, *C*). Calving speed is then less than the ice-flow speed.

[6] U.S. Geological Survey, 1201 Pacific Avenue–Suite 600, Tacoma, WA 98402

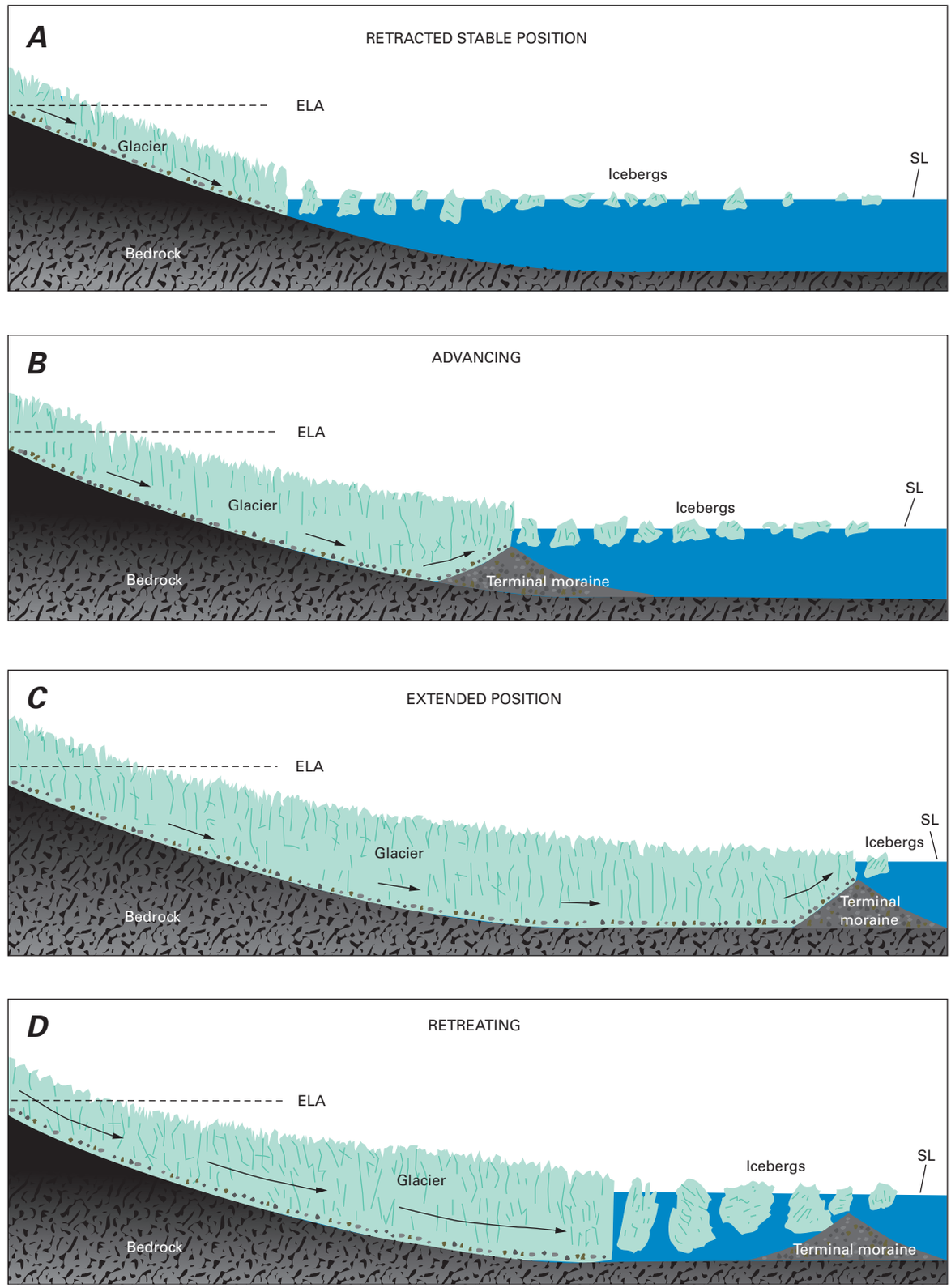

Figure 42.—*Tidewater-glacier cycle (from Trabant and others, 1990). Cross sections in* A *through* D *show four phases in the cycle.* **A** *shows the beginning and end of the cycle, when the glacier is located at the head of the fjord.* **B** *illustrates the advancing glacier moving the terminal moraine down fjord; and* **C** *the fully extended phase.* **D** *shows the retreating phase of the cycle, in which icebergs are much larger than those calved in the other three phases. The stable equilibrium line altitude (ELA) indicates that the tidewater-glacier cycle is relatively independent of climate change. Eustatic sea level (SL) is also stable.*

TABLE 2.—*Glaciological characteristics of existing (1–51) and former (52–60) tidewater glaciers of Alaska*
[Data in this table are from Viens (1995); * informal name proposed by Viens (1995). AAR, Accumulation area ratio.]

	Glacier name	length (km)	Total area[2] (km^2)	Accumulation area[3] (km^2)	Ablation area (km^2)	AAR
1.	McCarty	19.3	111	88	23	0.79
2.	Northwestern	12.1	60	54	6	0.89
3.	*Anchor**	4.8	7	5	2	0.77
4.	*Ogive**	6.8	9	6	2	0.73
5.	Holgate	12.9	69	63	6	0.92
6.	Aialik	12.9	70	62	8	0.88
7.	Chenega	24.1	369	346	23	0.94
8.	Tiger	11.3	56	50	6	0.89
9.	Nellie Juan	14.5	56	51	5	0.91
10.	Blackstone	12.1	32	29	2	0.92
11.	Beloit	10.1	25	24	1	0.95
12.	Harriman	12.9	60	48	13	0.79
13.	Surprise	12.1	80	64	16	0.80
14.	Barry	26.5	95	70	25	0.74
15.	Cascade	8.0	15	14	2	0.89
16.	Coxe	11.3	20	15	5	0.74
17.	Smith	9.7	20	16	4	0.81
18.	Bryn Mawr	7.6	26	22	4	0.84
19.	Wellesley	7.2	16	12	4	0.78
20.	Harvard	39.4	524	423	101	0.81
21.	Yale	32.2	194	153	41	0.79
22.	Meares	25.7	142	121	20	0.86
23.	Columbia	59.5	1,121	753	368	0.67
24.	Shoup	29.0	156	95	62	0.61
25.	Grotto-Moraine Apron	9.7	42	33	9	0.78
26.	Grotto-Moraine Apron		included in 25			
27.	Grotto-Moraine Apron		included in 25			
28.	Tsaa	20.9	150	144	70	0.96
29.	Guyot-Yahtse	64.4	1,432	1,368	64	0.96
30.	Guyot-Yahtse		included in 29			
31.	Tyndall	23.3	154	129	25	0.84
32.	Turner	31.8	186	150	36	0.81
33.	Hubbard	114.2	3,865	3,699	166	0.96
34.	Lituya	20.9	103	78	25	0.76
35.	North Crillon	20.1	71	57	13	0.81
36.	La Perouse	25.7	147	98	49	0.67
37.	Margerie	33.8	174	143	31	0.82
38.	Grand Pacific	60.3	654	459	195	0.70
39.	Reid	16.9	49	31	18	0.64
40.	Lamplugh	32.2	171	145	25	0.85
41.	Gilman	12.1	35	31	4	0.88
42.	Johns Hopkins	22.5	316	283	33	0.90
43	Kashoto	4.7	5	5	<1	0.94
44.	Hoonah	6.9	12	10	1	0.88

TABLE 2.—*Glaciological characteristics of existing (1–51) and former (52–60) tidewater glaciers of Alaska*

	Glacier name	length (km)	Total area[2] (km²)	Accumulation area[3] (km²)	Ablation area (km²)	AAR
45.	Muir	26.5	148	112	37	0.75
46.	Riggs	24.9	126	91	35	0.72
47.	McBride	24.1	143	84	59	0.59
48.	Sawyer	37.4	399	289	110	0.72
49.	South Sawyer	49.9	683	530	153	0.78
50.	Dawes	37.0	653	450	203	0.69
51.	LeConte	36.2	472	438	34	0.93
52.	Bainbridge	16.0	56	39	17	0.70
53.	Serpentine	10.0	30	21	9	0.70
54.	Bering	191.0	5,173	3,213	1,961	0.62
55.	Malaspina	108.0	5,008	2,575	2,433	0.51
56.	Nunatak	34.0	312	182	131	0.58
57.	Brady	51.0	590	382	208	0.65
58.	Carroll	49.0	527	387	140	0.73
59.	Taku	60.0	831	728	102	0.88
60.	Baird	50.0	784	527	257	0.67

[1.] Multiple appearances of the same name (that is, Grotto-Moraine Apron and Guyot-Yahtse) indicate a single glacier with more than one tidewater face.
[2.] Total area of the 60 tidewater glaciers is 26,834 km² or approximately 35 percent of the glacierized area of Alaska.
[3.] Total accumulation area of the 60 tidewater glaciers is 19,821 km².
[4.] The average AAR for these 60 glaciers is 0.74.

TABLE 3.—*Terminus status of major tidewater glaciers of Alaska in 1999 (with status in 2004 added for selected glaciers)*
[See figure 41, this volume. na, not available.]

Glacier	Lat. (N)[1]	Long.(W)[1]	Area (km²) [1]	Median ELA (m amsl) [1,2]	Terminus position[1,3]	Status of terminus in 1999 (from Robert M. Krimmel, except where noted)	Terminus status in 2004[3,6]
Kenai Mountains Group							
McCarty	59°50'	150°13'	111	991	Advance rate decreased between 1985 and 1995	Very slow advance since 1960 in shallow water at head of McCarty Fiord	Ret.
Northwestern	59°52'	150°5'	60	976	R	Stable at head of Northwestern Fiord	Ret.
Anchor[1]	59°46'	150°5'	7	991	na	Stable[1]	Slowly Ret.
Ogive[1]	59°47'	150°5'	9	1,204	na	Stable[1]	Slowly Ret.
Holgate	59°52'	149°54'	69	610	R	Stable at head of Holgate Arm	Slowly Ret.
Aialik	59°53'	149°49'	70	732	R	Stable at head of Aialik Bay	–
Bainbridge[5]	60°7'	148°27'	565	5645	R[4], FTW[5]	Stable[5]	–
Tiger	60°11'	148°30'	56	518	R	Stable at head of Icy Fiord	–
Chenega	60°17'	148°28'	369	534	R	Stable at head of Nassau Fiord	Slowly Ret.
Nellie Juan	60°26'	148°25'	56	396	I	Drastic retreat in narrow inlet, Derickson Bay	–
Blackstone	60°39'	148°44'	32	503	R	Stable at head of Blackstone Bay	Slowly Ret.
Beloit	60°38'	148°43'	25	473	R	Stable at head of Blackstone Bay	Slowly Ret.
Chugach Mountains Group							
Harriman	60°56'	148°31'	60	427	I	Extended position on moraine exposed at low tide in Harriman Fiord	Slowly Adv.
Surprise	61°3'	148°29'	80	854	R	Stable at head of Surprise Inlet	Slowly Ret.
Cascade	61°8'	148°12'	15	945	I	Stable on beach, Harriman Fiord	Slowly Ret.
Coxe[1]	61°8'	148°3'	20	1,006	R	Stable[1]	Slowly Ret.

TABLE 3.—*Terminus status of major tidewater glaciers of Alaska in 1999 (with status in 2004 added for selected glaciers)*

Glacier	Lat. (N)[1]	Long.(W)[1]	Area (km^2)[1]	Median ELA (m amsl)[1,2]	Terminus position[1,3]	Status of terminus in 1999 (from Robert M. Krimmel, except where noted)	Terminus status in 2004[3,6]
Serpentine[5]	61°7'	148°17'	305	8545	R[4], FTW[5]	Slow retreat[5]	–
Barry	61°12'	148°2'	95	1,021	R	Stable at head of Barrry Arm	–
Wellesley	61°7'	147°56'	16	1,037	na	Stable on beach, College Fiord	Rapidly Ret.
Bryn Mawr	61°17'	147°48'	26	1,006	na	Stable on beach, College Fiord	Slowly Ret.
Smith	61°15'	147°50'	20	976	na	Stable on beach, College Fiord	Slowly Ret.
Harvard	61°23'	147°23'	524	1,098	I	Slow advance on terminal moraine shoal, College Fiord	–
Yale	61°18'	147°27'	194	1,098	R	Drastic retreat, or stable at head of Yale Arm	Slowly Ret.
Meares	61°13'	147°27'	142	1,052	I	Slow advance on terminal moraine shoal at head of Unakwik Inlet	Same as 1999
Columbia	61°15'	146°54'	1,121	899	I	Drastic retreat, fore bay, Columbia Bay	Same as 1999
Shoup	61°14'	146°28'	156	1,037	I	Drastic retreat in tidal basin, Shoup Bay	Same as 1999
Bering[5]	60°30'	142°24'	5,1735	1,0375	R[4], FTW[5]	Drastic retreat[5]	Same as 1999
St. Elias Mountains Group							
Grotto	60°3'	141°33'	42	701	R	Stable on beach, Tsaa Fiord	Slowly Ret.
Moraine/Apron					R	Stable on beach, Tsaa Fiord	Slowly Ret.
Tsaa	60°7'	141°37'	150	625	R	Stable at head of Tsaa Fiord	Slowly Ret.
Guyot	60°13'	141°22'	1,432	747	R	Stable at head of Icy Bay	Ret.
Yahtse					R	Stable at head of Icy Bay	Ret.
Tyndall	60°13'	141°5'	154	915	R	Stable at head of Taan Fiord	–
Malaspina[5]	60°6'	140°30'	5,0085	8235	R[4], FTW[5]	Stable[5]	Rapidly Ret.
Disenchantment Bay Group							
Turner	60°5'	139°45'	186	854	na	Advances to terminal moraine shoal during surges	At shoal
Hubbard	60°10'	139°30'	3,865	915	I	Slow advance on terminal moraine shoal, Disenchantment Bay	Same as 1999
East Nunatak[4] (Nunatak[5])	59°42'	138°3'	3125	1,0525	R[4], FTW[5]	Stable at head of Nunatak Fiord, no longer calves icebergs	Ret.
Fairweather Range Group							
Lituya	58°44'	137°26'	103	1,052	I	Stable on terminal moraine shoal, Lituya Bay	Adv.
North Crillon	58°40'	137°19'	71	991	I	Stable on terminal moraine shoal, Lituya Bay	Adv.
La Perouse	58°32'	137°13'	147	960	na	Stable on open beach in Gulf of Alaska	Same as 1999
Reid	58°46'	136°48'	49	732	R	Stable at head of fiord, Reid Inlet	Slowly Ret.
Lamplugh	58°48'	136°52'	171	701	R	Stable on beach, Johns Hopkins Inlet	Same as 1999
Gilman	58°48'	137°3'	35	838	na	Stable on beach, Johns Hopkins Inlet	Adv.
Johns Hopkins	58°47'	137°12'	316	747	I	Advancing on terminal moraine shoal, Johns Hopkins Inlet	Same as 1999
Margerie	58°58'	137°14'	174	1,067	na	Stable on beach, Tarr Inlet	Same as 1999
Grand Pacific	59°6'	137°27'	654	1,189	I	Slow advance on terminal moraine shoal at head of Tarr Inlet	Rapidly Ret., stagnant ice
Kashoto[1]	58°52'	137°2'	5	762	na	Stable[1]	Ret.
Hoonah[1]	58°50'	137°4'	12	793	na	Stable[1]	Ret.
Brady[5]	58°33'	137°45'	5905	6105	R[4], FTW[5]	Stable[1]	Ret.

TABLE 3.—*Terminus status of major tidewater glaciers of Alaska in 1999 (with status in 2004 added for selected glaciers)*

Glacier	Lat. (N)[1]	Long.(W)[1]	Area (km^2) [1]	Median ELA (m amsl) [1,2]	Terminus position[1,3]	Status of terminus in 1999 (from Robert M. Krimmel, except where noted)	Terminus status in 2004[3,6]
Alsek Range Group							
Muir	59°10'	136°28'	148	960	R	Stable at head of fiord, Muir Inlet, no longer calves icebergs	400 m inland from shoreline, stagnant ice
Riggs	59°8'	136°14'	126	960	R	Stable on beach, Muir Inlet	Ret.
McBride	59°10'	136°5'	143	1,189	I	Stable at head of tidal inlet, Muir Inlet	Rapidly Ret.
Carroll[5]	59°11'	136°40'	5275	9915	R[4], FTW[5]	Stable[5]	Debris-covered, stagnant ice
Coast Mountains Group							
Taku[4,5]	58°36'	134°9'	8315	8995	R[4], FTW[5]	Stable on river bar/terminal moraine, Taku Inlet, no longer calves icebergs. Viens[5] indicated that it had been advancing at a decreased rate	Same as 1999
Sawyer	57°53'	132°55'	399	1,372	R	Retreat in narrow inlet, Tracy Arm	Same as 1999
South Sawyer	57°45'	132°43'	683	1,372	I	Stable in narrow inlet, sharp bend, Tracy Arm	Same as 1999
Dawes	57°27'	132°30'	653	1,402	I	Drastic retreat in narrow, deep inlet, Endicott Arm	Same as 1999
LeConte	56°54'	132°22'	472	915	R	Drastic retreat in narrow, deep inlet, LeConte Bay	Same as 1999
Baird[5]	57°15'	132°21'	7845	1,2345	R4, FTW[5]	Stable[5]	Same as 1999

[1] Viens (1995, table A1).
[2] Meters above mean sea level.
[3] R, Retracted; I, Intermediate; Ret., Retreating; Adv., Advancing.
[4] From Robert M. Krimmel (written commun., 1999).
[5] Classified by Viens (1995, table A2) as a former tidewater (FTW) calving glacier.

Examples of tidewater glacier instability abound in Alaska. During the 20th century, most of the glaciers in Glacier Bay ended a drastic retreat of nearly 100 km that began about 200 years ago. Johns Hopkins Glacier, in western Glacier Bay, began a slow readvance early in the 20th century, while Muir Glacier in eastern Glacier Bay continued its retreat through the present. Glaciers in Icy Bay began a retreat from an extended position early in the 20th century and had retreated 30 km by late in the century. Hubbard Glacier has generally advanced during the 20th century; it advanced rapidly across a major fjord in May 1986 and created an ice-dammed lake that drained catastrophically (jökulhlaup), but harmlessly, in October 1986. A similar event occurred in the summer of 2002 (see section on "The 1986 and 2002 Temporary Closures of Russell Fiord by the Hubbard Glacier" in this chapter). Columbia Glacier began a rapid retreat during 1982 that continued into the 21st century. Columbia Glacier, the most intensively studied tidewater glacier in the world, is of particular interest because its discharge of icebergs into shipping lanes of Prince William Sound constitutes a hazard to navigation.

Columbia Glacier

The Columbia Glacier (about lat 61°N., long 147°W.) (figs. 43–46) is a calving glacier that terminates in an embayment (forebay) of Prince William Sound, near Valdez, Alaska; it has an area of about 1,000 km^2. The glacier is currently undergoing a rapid retreat from what had been a stable position for more than two centuries prior to 1980 (Vancouver, 1798). Ice mass is lost from the Columbia Glacier predominately through the calving of icebergs from its tidewater terminus. Some of the icebergs float into the shipping lanes that are used by oil tankers traveling to or from the port of Valdez, the

Figure 43.—*Two oblique aerial photographs of the Columbia Glacier, Chugach Mountains.* **A**, *By 22 August 1979, large embayments formed in the terminus, and the glacier had receded from Heather Island (foreground), where a stagnant ice mass still remained.* ► **B**, *By 12 September 1986 there had been more than 2 km of retreat. The moraine shoal, where the water was no deeper than 21 m, is marked by stranded icebergs, which tend to keep the concentrated brash ice contained in the forebay between the terminus and moraine. Water depth in the forebay is 200 to 300 m. The rapid retreat will continue for several decades and will not end until the fjord head is reached in the east branch (right side). Photograph Nos. 79–L2–028 and 86–R2–256 by Austin Post, and Robert M. Krimmel, respectively, U.S. Geological Survey. Caption courtesy of Robert M. Krimmel, U.S. Geological Survey.*

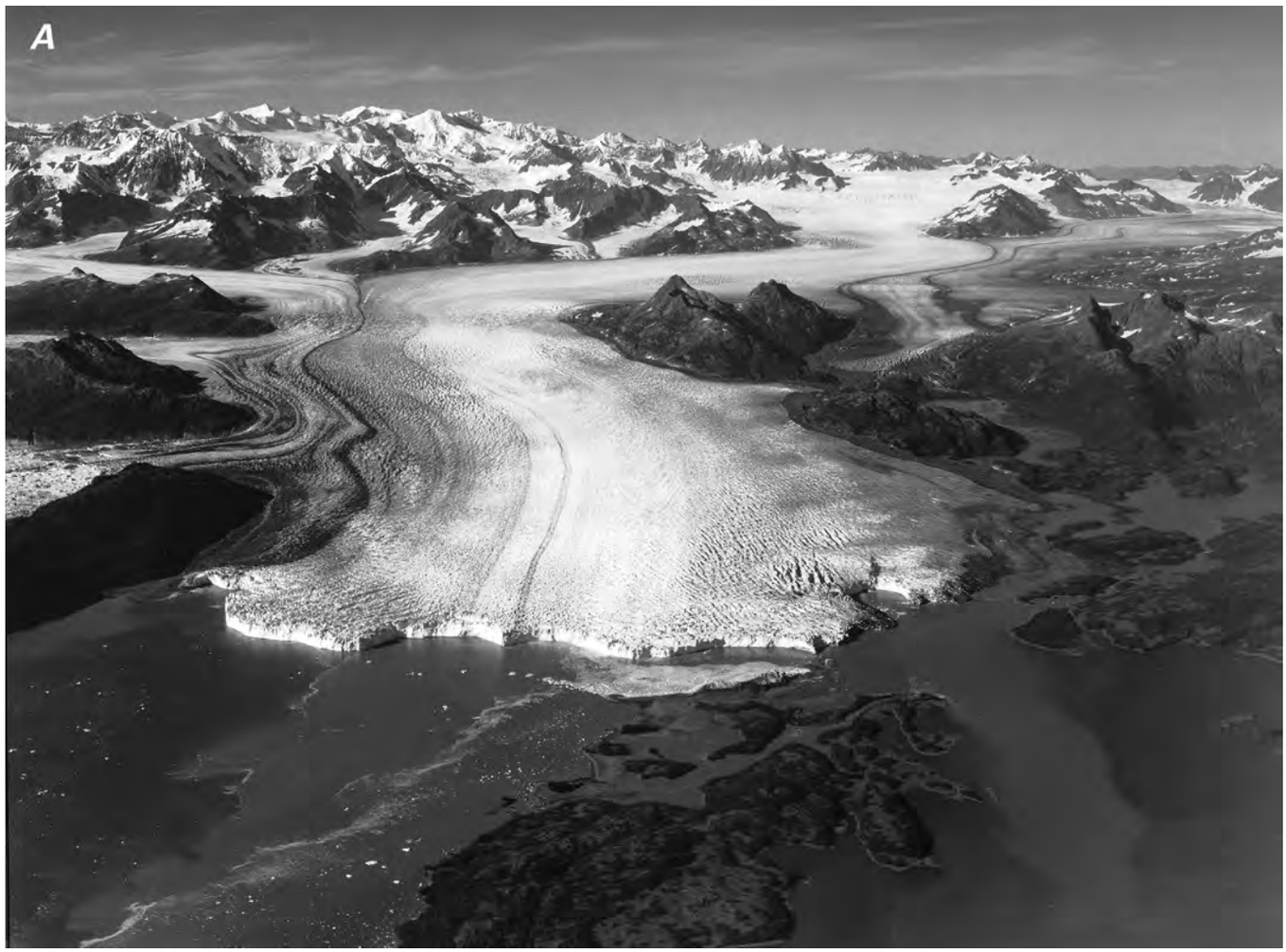

southern terminus of the Trans-Alaska [oil] Pipeline. Although the glacier terminates in tidewater, Columbia Glacier is grounded on its bed because the ice thickness overcomes buoyancy. In places, the glacier bed lies as much as 550 m below sea level (Meier and others, 1994). Flotation of the glacier may take place for brief periods in localized areas near the calving face.

The retreat of Columbia Glacier is interesting because it provides an opportunity for glaciologists to study the processes involved in iceberg calving and movement (Meier, 1994, 1997; Kamb and others, 1994), the ice dynamics of a rapidly changing system, a modern-day analog of suspected past rapid glacier retreats, and the processes associated with marine-based ice-sheet disintegration (for example, the marine-based part of the Antarctic ice sheet in West Antarctica) (see Swithinbank, 1988). Iceberg production during this retreat is important to shipping interests because icebergs are a navigation hazard. The tourist industry is interested because calving glaciers and icebergs are natural attractions in Prince William Sound.

A large part of the scientific studies of Columbia Glacier has been documenting the changes associated with its retreat (Rasmussen and Meier, 1982, 1985; Sikonia, 1982; Bindschadler and Rasmussen, 1983; Brown and others, 1982, 1986; Meier and others, 1985, 1994; Walters and Dunlap, 1987;

Rasmussen, 1989). This documentation has been done at a variety of temporal and spatial scales. For instance, ice displacement at a few places has been measured by using automated, laser-ranging devices with centimeter accuracy at a 10-minute frequency (Walters and Dunlap, 1987; Meier and others, 1994). [Editors' note: According to Mark F. Meier (written commun., 2004), the results of these studies showed the short-term response of the glacier to daily melt cycles, precipitation events, and even the changing pressure on the subglacier water system caused by ocean tides and thereby defined glacier-sliding processes.] At the synoptic scale, Landsat imagery has been used to observe the extent of iceberg plumes emanating from the glacier (fig. 45). Geodetic surveying is labor intensive and focuses on very specific

Figure 44.—*Oblique aerial photograph of Columbia Glacier on 10 January 1993, from about 7,000 m in altitude, looking approximately north, with the iceberg-filled forebay in the foreground. At the time of the photograph, the glacier was undergoing a rapid retreat; the accelerated retreat produced the large number of icebergs (see fig. 42*D*). Photograph No. 93–V1–39 by Robert M. Krimmel, U.S. Geological Survey.*

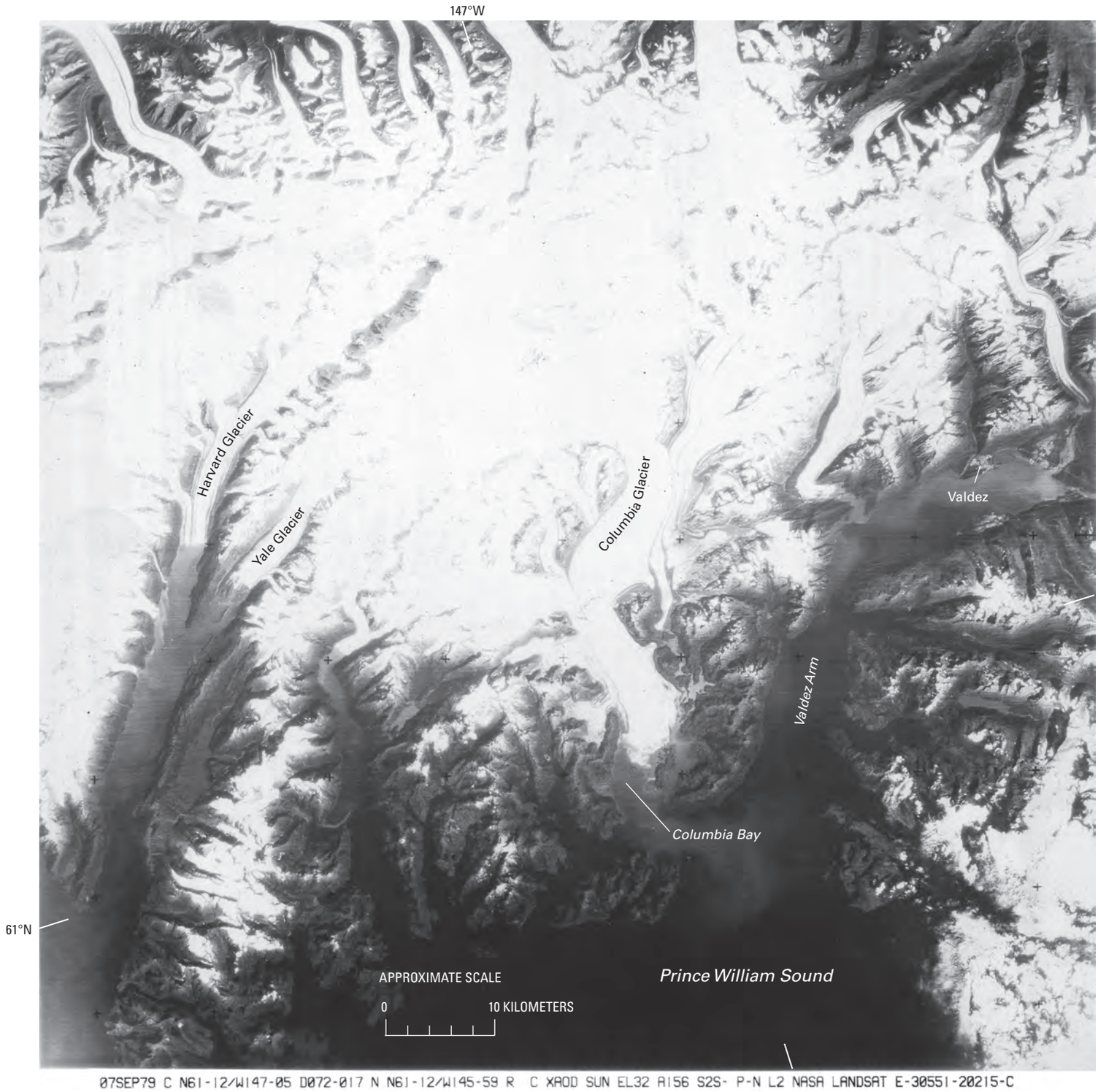

Figure 45.—*Landsat 3 RBV image of Columbia Glacier and a part of Prince William Sound. The plume of icebergs caused by calving can be seen extending from Columbia Bay into Valdez Arm and Prince William Sound. Landsat 3 RBV image (30551–20215–C; 7 September 1979; Path 72, Row 17), originally published by Krimmel and Meier (1989), is from the USGS, EROS Data Center, Sioux Falls, S. Dak.*

goals. Satellite images do not offer sufficient detail for many purposes and are dependent on weather (cloud cover) and orbit (frequency of imaging). The most practical method for documenting the changes at Columbia Glacier has proven to be repetitive aerial photography (Meier and others, 1985).

Oblique and vertical aerial photography has been used routinely to study Columbia Glacier since 1960, when Austin Post (USGS) began near-annual observations of Columbia Glacier as part of broad-coverage aerial surveys of Alaskan glaciers. Post documented glacier conditions with a large-format (9-in [23-cm] film) metric camera that could be mounted to acquire either oblique or vertical aerial photography. By the early 1970s, Post had become aware that Columbia Glacier was the only major tidewater glacier in Alaska that was neither retreating nor advancing. As mentioned previously, the tidewater glaciers of Glacier Bay had been undergoing a major retreat during the last two centuries; Hubbard Glacier was advancing slowly, and the glaciers in Icy Bay had retreated rapidly since about 1930. Post (1975) published a report that described changes in the terminus of Columbia Glacier and suggested that the increasing size and frequency of seasonal embayments in the terminus might be a precursor to a more rapid retreat. Summer and fall retreats of the terminus from a terminal-moraine shoal, where the water was mostly less than about 20 m deep, were normally offset by the subsequent winter and spring advances. But what if the winter and spring readvances did not occur? In 1976, the USGS systematically began to obtain aerial photographs of the lower reach of Columbia Glacier to document the changes. This photography enabled accurate monitoring and mapping of the retreat (fig. 46) (Krimmel, 1987, 2001).

Repeated stereo aerial photography covered the lowest 20 km of the glacier at a spatial scale that allowed a single frame to span the entire width of the glacier and include off-glacier geodetic ground-control points along both edges of the flight line (fig. 46). A 6-in (15.3 cm) focal-length lens, metric camera, with 9-in (23 cm) film, flown at 7,000 m in altitude yielded the required coverage with six overlapping frames. (The overlap was at least 60 percent to achieve stereoscopy.) The temporal scale was designed so that ice features were preserved from one survey flight to the next. Thus, seasonal changes of the terminus position and ice speed were documented. By 2000, photography of the lower reach had been acquired 120 times. Flight frequency was controlled by scientific requirements, weather, logistics, and project funding. The shortest interval between flights was 3 days; the longest was 330 days. On 20 flights, coverage was extended to include areas beyond the lower reach of the glacier.

Stereophotogrammetry

Analytical stereophotogrammetric techniques were used to analyze the vertical aerial photographs of Columbia Glacier.

Terminus position. Normally a well-defined ice cliff is formed where glacier ice calves into a lake or the ocean, and the terminus can be identified easily at many points along the ice-water contact. At times, the Columbia Glacier ice cliff is so low that it is difficult to define the contact between water and glacier; in those areas the position was estimated.

Figure 46.—*Reduced-scale mosaic of five vertical aerial photographs of the lower reach of the Columbia Glacier on 2 October 1998 from an altitude of about 7,000 m. North is approximately at the top; the terminus of the glacier is about 4 km wide. Superimposed on the mosaic are plots of selected terminus positions from 1981 to 1999. Also shown by symbol are three locations where the velocity of the glacier surface was determined. Glacier surface speeds are shown in figure 49. The scale of the original U.S. Geological Survey (USGS) aerial photographs is about 1:46,000 at sea level. The current scale is approximately 1:100,000. USGS Columbia Glacier aerial photographs are referenced as: 10–2–98; 23,000 feet; Frames 1–3 through 1–7.*

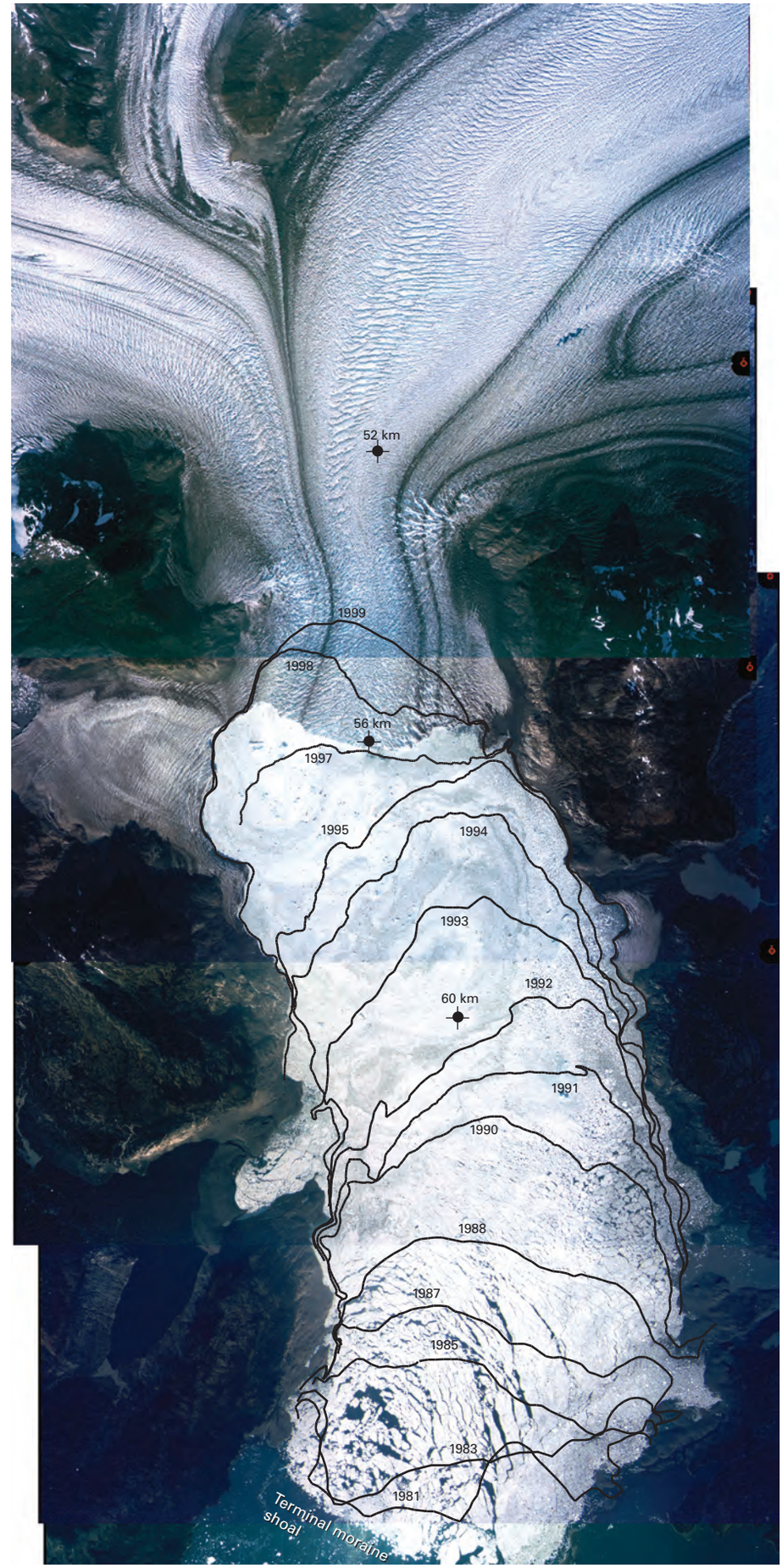

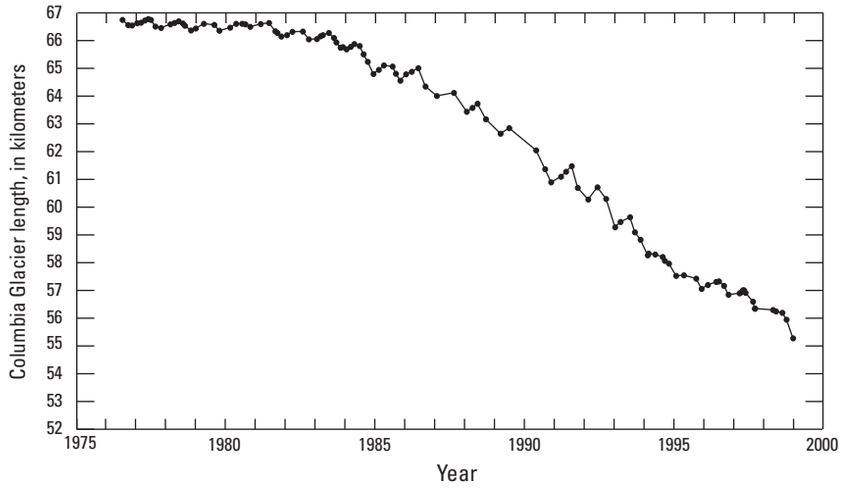

Figure 47.—*The changing length of Columbia Glacier between 1976 and 1999. Each dot represents an aerial survey. When the recessional trend is removed, the seasonal variations shown in figure 48 become evident.*

The width-averaged (one-dimensional) terminus position in terms of glacier length is plotted in figure 47. The glacier length plot shows that the major recession began about 1982 (slowly at first) and then increased to a rate of about 0.7 km a^{-1} until 1995, when the recession rate decreased until 1998. In the last years of the 20th century, there was a marked increase in the rate of retreat (Pfeffer and others, 2000). During the end of 1998, the retreat rate increased to nearly 1.0 km a^{-1}, and in 2004 it had decreased to 0.6–0.7 km a^{-1} (Mark F. Meier, written commun., 2004).

The persistent change in the terminus position is seasonal. The glacier terminus is extended during the winter and spring, and the terminus retreats in summer and fall. This seasonal cycle of change in glacier length is shown in figure 48.

Ice speed. The highly crevassed lower reach of Columbia Glacier lends itself to measurements by aerial-stereophotogrammetric methods (fig. 49). An individual crevasse or local pattern of crevasses retains its unique geometric identity for days, in some cases for months, and in some rare areas for several years. These intervals allow sufficient time for photographic-identification of features and measurement by means of stereophotogrammetic methods. Displacements of these features can be converted to speeds by dividing the displacement by the time interval. Such measurements can be made over the entire lower reach of Columbia Glacier if the time interval between survey flights is short enough that the features or crevasse patterns on the aerial photographs remain identifiable.

Before the Columbia Glacier began to retreat, features or crevasse patterns could be followed over the entire lower reach for periods of up to 4 months. By the middle 1980s, the ice speed and rate of deformation had increased to such an extent that features within a few kilometers of the terminus could be reidentified only within intervals of a few weeks or less. In the spring of 1997, five aerial photography sets obtained at intervals of 10 to 20 days allowed detailed spatial and temporal speed measurements to be made.

The glacier speed has increased severalfold since the retreat began. Before the retreat, the maximum annual ice speed averaged about 5 m d^{-1}, the seasonal maximum speed being about 7 m d^{-1}. The speed increased differentially in the lower reaches of the glacier, the greatest increase occurring near the terminus (fig. 49). As the retreat progressed, speed near the terminus increased to more than 20 m d^{-1} averaged annually (fig. 50) and reached 30 m d^{-1} during the seasonal speed maximum. The seasonal speed variation

Figure 48.—*The seasonal variation of the length of Columbia Glacier. Deviations from the normalized length (best fit curve) are plotted against the time of year. The numerals indicate the survey year (76=1976).*

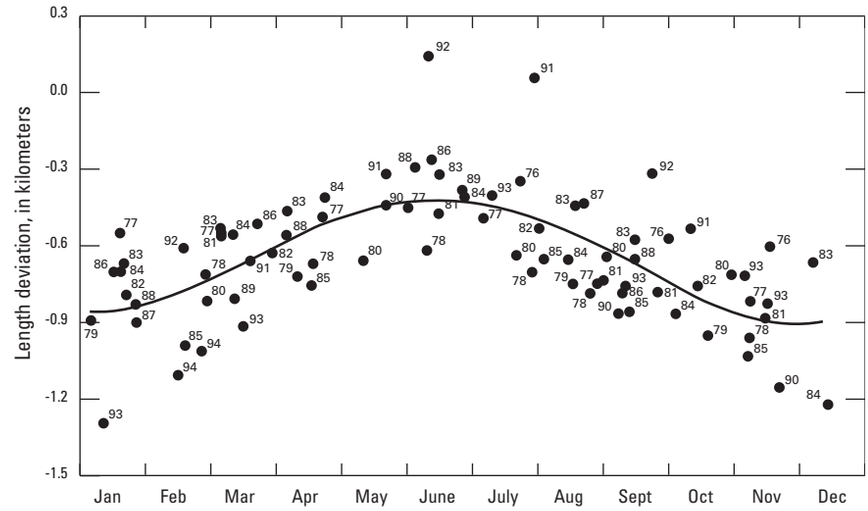

Figure 49.—*Surface speed of Columbia Glacier at three locations, 52 km (black), 56 km (blue), and 60 km (red), from the origin (head) of the glacier on different aerial survey dates from 1977 to 1997. The location where the velocities were determined is shown on figure 46.*

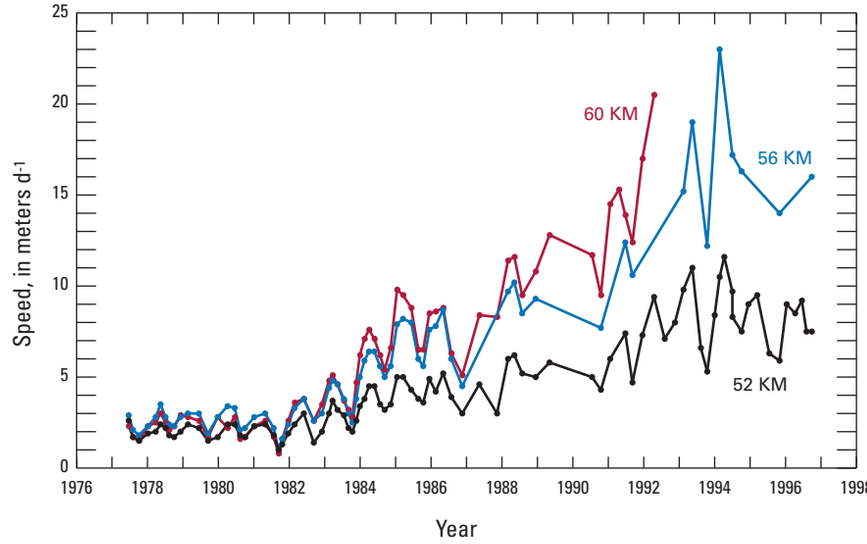

Figure 50.—*Average annual speed in meters per day along the length of Columbia Glacier in 1978 and 1993. The fourfold increase in speed near the terminus is evident.*

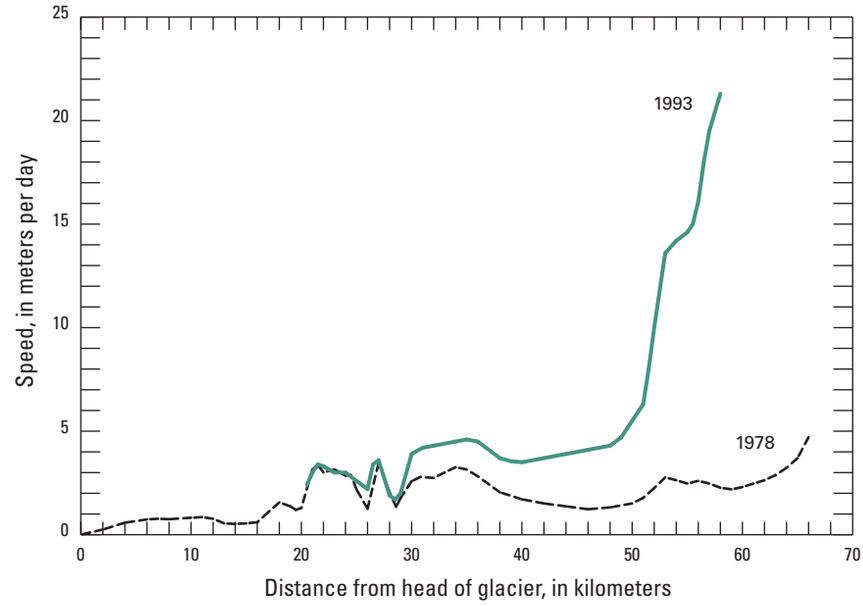

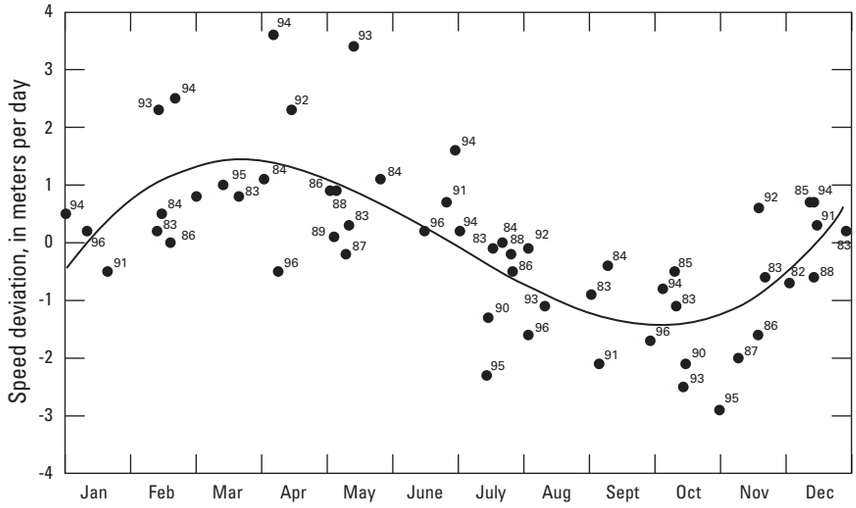

Figure 51.—*The seasonal-speed deviations from the normalized speed (best fit curve) near the terminus of Columbia Glacier. Speed is highest in early spring and lowest in early fall. The numerals indicate the year (84=1984).*

near the terminus is shown in figure 51, where deviations from the normalized speed (the long-term trend removed) are plotted against the time of year. Speed is highest in early spring and lowest in early fall.

Ice displacement also has been measured very precisely, with a temporal resolution of less than 1 hour for several multiple-week periods at a few locations. Ice speed fluctuated daily, the highest speed occurring about 8:00 p.m. and the lowest at about 8:00 a.m. In addition, speed reached high extremes near the end of rain or wind storms. High glacier speed seemed to correlate with measured or assumed high basal-water pressure or volume of water in storage at the bed, depending on the time scales of the fluctuations (Meier and others, 1994; Kamb and others, 1994). Within 1.5 km of the terminus, the stage of the tide also affected ice speed. When there was little or no surface water input by melt or precipitation, glacier speed had an inverse relation to tide stage. The increased pressure of high tide against the ice cliff slowed the glacier slightly (Krimmel and Vaughn, 1987; Walters and Dunlap, 1987) and overwhelmed any speed increase that may have occurred because of a local increase in basal pressure owing to high tide.

Forebay of Columbia Glacier. As Columbia Glacier has retreated, the fjord has lengthened. Except for a narrow band along each side of the glacier, the glacier bed has been below sea level throughout the area of the retreat. Thus, fjord expansion is nearly equal in area to glacier retreat. As the glacier has retreated, the surface of the newly opened fjord, presently known as the forebay, usually has been covered with a floating mass of icebergs, brash ice, and frozen fresh-water ice. This "freeze-welded" sheet has covered almost all of the forebay most of the time during the retreat (fig. 44). The southern limit of the forebay is the terminal moraine shoal, which was the stable position of the terminus of Columbia Glacier before the beginning of the retreat. Maximum water depth over the moraine was 27 m at high tide in the middle 1980s. The northern end of the forebay is the glacier terminus. The forebay ice mass is continuously replenished by newly calved ice and moves toward the terminal moraine at a rate of about 100 m d^{-1}. The ice mass in the forebay undergoes little transverse mixing. As a result, the relatively debris-laden icebergs calved from the medial moraine retain their transverse position as they move through the forebay (fig. 44).

Beginning in late 1995, the floating ice mass in the forebay occasionally thinned enough so that boats could approach the glacier terminus. Shipborne bathymetric measurements indicate that the maximum fjord water depth was about 360 m and that submarine topographic features were up to 100 m in relief (Post, 1997).

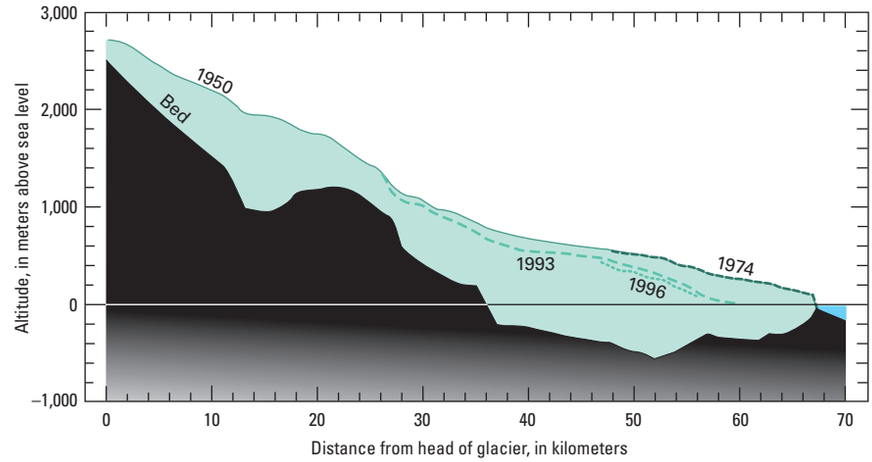

Figure 52.—*Surface altitude of Columbia Glacier in 1950, 1974, 1993, and 1996, with an estimated width-averaged bed. The lower part of the glacier has thinned at a rate of about 20 m a^{-1}.*

Ice-surface altitude. The surface altitude of points on stereophotogrammetric models is measured easily. It is more difficult to obtain a consistent area-averaged ice-surface altitude. Ice surface relief is typically 20 to 30 m. This roughness must be smoothed to give meaningful measurements of changes in ice-surface altitude. The surface altitude has been reduced during retreat.

The lower part of Columbia Glacier has thinned at a rate of about 20 m a^{-1}. The magnitude of thinning decreases up glacier, reaching approximately zero about 26 km from the head of the glacier (fig. 52).

Calving. Calving is the breaking off of ice from the terminus of a glacier. If the terminus position of a calving glacier is stable, the calving rate is equal to the ice speed. If the terminus is retreating, the calving rate is equal to the ice speed plus the retreat rate. Calving is rarely observed directly on aerial photographs. It is normally measured by the difference between the observed glacier speed and the change in terminus position. Calving can also be measured directly between two observation dates by delineating the area of ice that is present near the terminus on the first date but is missing on the second date. By measuring the area of "ice to be-calved" and the average altitude of its top surface, and by estimating the ice thickness, one can determine a calving volume. Applying this analysis to Columbia Glacier indicates that the calving rate has increased by a factor of 5 or more since the retreat began and that, during the retreat, it has often been as high as 5 km^3 a^{-1}. During the years 2001–03, the calf-ice discharge approached 10 km^3 a^{-1} (O'Neel and others, 2005).

Discussion. The high ice-surface velocities measured at Columbia Glacier rival those measured at glaciers during surges (Kamb and others, 1985). However, the condition of Columbia Glacier is unlike that of a typical surging glacier in two ways. First, high ice speed at a surging glacier occurs during a shorter period; a typical large surging glacier has one or more short periods of high speed lasting a few months and a period of several decades when speeds are "normal" (50–200 m a^{-1}). The high ice speed of Columbia Glacier has been sustained for more than a decade. Second, a surge usually begins upglacier, well above the terminus (often in the accumulation zone), and it propagates downglacier. No propagation of a speed pulse downglacier has occurred at Columbia Glacier. The only longitudinal effect is that ice drawdown and ice speedup are progressing upglacier (Meier and others, 1985; Pfeffer, 2007). Thus, the term "surge" should not be applied to the flow regime of Columbia Glacier.

The seasonal velocity variations of Columbia Glacier—fast in the early spring and slow in the fall—are consistent with those of many other glaciers and can be explained as seasonal variations in the basal-water pressure at the glacier-bed interface (Kamb and others, 1994). The dominant mechanism of movement of Columbia Glacier must be basal sliding (Rasmussen, 1989; Kamb and others, 1994), for which Bindschadler (1978) has devised a general

ice-flow law, although some of its parameters remain in doubt. A qualitative description of the basal-sliding process depends on basal-water pressure and storage of water. Basal-water pressure is controlled by a channel network at the bed, which may be opened (allowing for water passage) or closed (resulting in water storage). During the summer, sufficient water is available from ice melt and rain to keep many basal channels open despite their tendency to be closed by ice deformation. Basal-water pressure in the summer is therefore low. In the fall, surface melting is reduced, and precipitation is increasingly dominated by snow; basal-water pressure is at an annual minimum as the water input diminishes. Basal sliding and deformation gradually disrupt the channel system. Once the channels are disrupted, no more water can pass under the glacier, and residual water draining from the glacier surface, intraglacier conduits, and the surrounding subglacier basin is stored. Basal-water pressure increases throughout the winter and well into the spring. Ultimately, however, water pressure becomes high enough to force channels to open and remain open owing to the high volume of water moving through and under the glacier. Glacier speed is a direct function of basal-water thickness and pressure. Consistent with this explanation, short-term measurements show that speed has a strong diurnal variation that is directly related to diurnal water input (Kamb and others, 1994) and summer precipitation events.

Although the cause of seasonal ice-speed variations is agreed upon generally, the cause of decadal-scale increases in speed is not understood. One hypothesis is that a feedback exists, in which decreasing ice thickness causes reduced effective pressure at the bed, which in turn allows increased sliding; this process reduces the ice thickness, and further reduces effective pressure (Meier and Post, 1987; Meier, 1994). Another hypothesis is that a change in the bulk characteristics of the glacier ice results in lower tensional strength and increased speed. How the process of calving works, how it is related to changes in speed, and, perhaps, how calving influences speed are open questions (van der Veen, 1995, 1996, 1997b) and were discussed in a workshop focusing on these questions (Van der Veen, 1997a).

Hubbard Glacier

Hubbard Glacier (about lat 60°N., long 139°30'W.) (fig. 53) is the largest tidewater glacier in Alaska and has been generally advancing (figs. 54, 55, 56) since it was first mapped by the International Boundary Commission (IBC) in 1895 (Davidson, 1903). The advance has accelerated during the 20th century at the following average advance rates: 1895–1948, 16 m a^{-1}; 1948–62, 18 m a^{-1}; 1962–72, 30 m a^{-1}; 1972–83, 38 m a^{-1}; and 1983–88, 47 m a^{-1} (Trabant and others, 1990). This slow advance led Post and Mayo (1971) to predict that Hubbard Glacier would dam Russell Fiord by 1990. The overall advance is persistent but varies locally over the 10-km width of the terminal ice cliff. Hubbard Glacier often exhibits short-lived pulses characterized by much higher advance rates. Although these pulses usually occur in the spring, it is not known whether they occur every spring or how much of the terminus they affect. In 1986, one such pulse was directed across the mouth of Russell Fiord and resulted in a temporary closure. The advancing ice was protected by a ridge of moraine material that the glacier pushed ahead of itself, and calving was thus effectively reduced. By the end of May, the entrance to the fjord was closed (fig. 56). When the closure (fig. 56) was completed, the level of the "lake" in Russell Fiord began rising from spring snowmelt and precipitation runoff. A far-reaching concern was the possible overflow from the south end of *Russell Lake* and the effect that such an overflow would have on the productive fishery in the Situk River basin. Overflow would have occurred when the lake level reached 40 m, but, on 7 October 1986, at a water level of 25 m, the ice dam failed, and *Russell Lake* drained catastrophically (jökulhlaup) but harmlessly into Disenchantment Bay (Mayo, 1988b). Temporary closure occurred again in 2002. For a further

***Figure 53.**—Digitally enhanced Landsat 5 TM image of Hubbard Glacier. Hubbard Glacier has been generally advancing since 1895. The Landsat 5 TM image (50620–18008; bands 2, 3, 4; 7 August 1985; Path 62, Row 18) is from the USGS, EROS Data Center, Sioux Falls, S. Dak. (Also available in EROS Data Center Image Gallery: No. E–564–99CT.)*

discussion of the closures, see the section on "The 1986 and 2002 Temporary Closures of Russell Fiord by the Hubbard Glacier" in the following discussion of the St. Elias Mountains.

Although the closure of Russell Fiord is unique to present-day inhabitants of the area, it is known to have occurred in the past. Native legends refer to events that may have been the result of closure. The channel of the Situk River on the southern end of Russell Fiord is larger than necessary, so that it can handle the discharge when the fjord is not open to Disenchantment Bay.

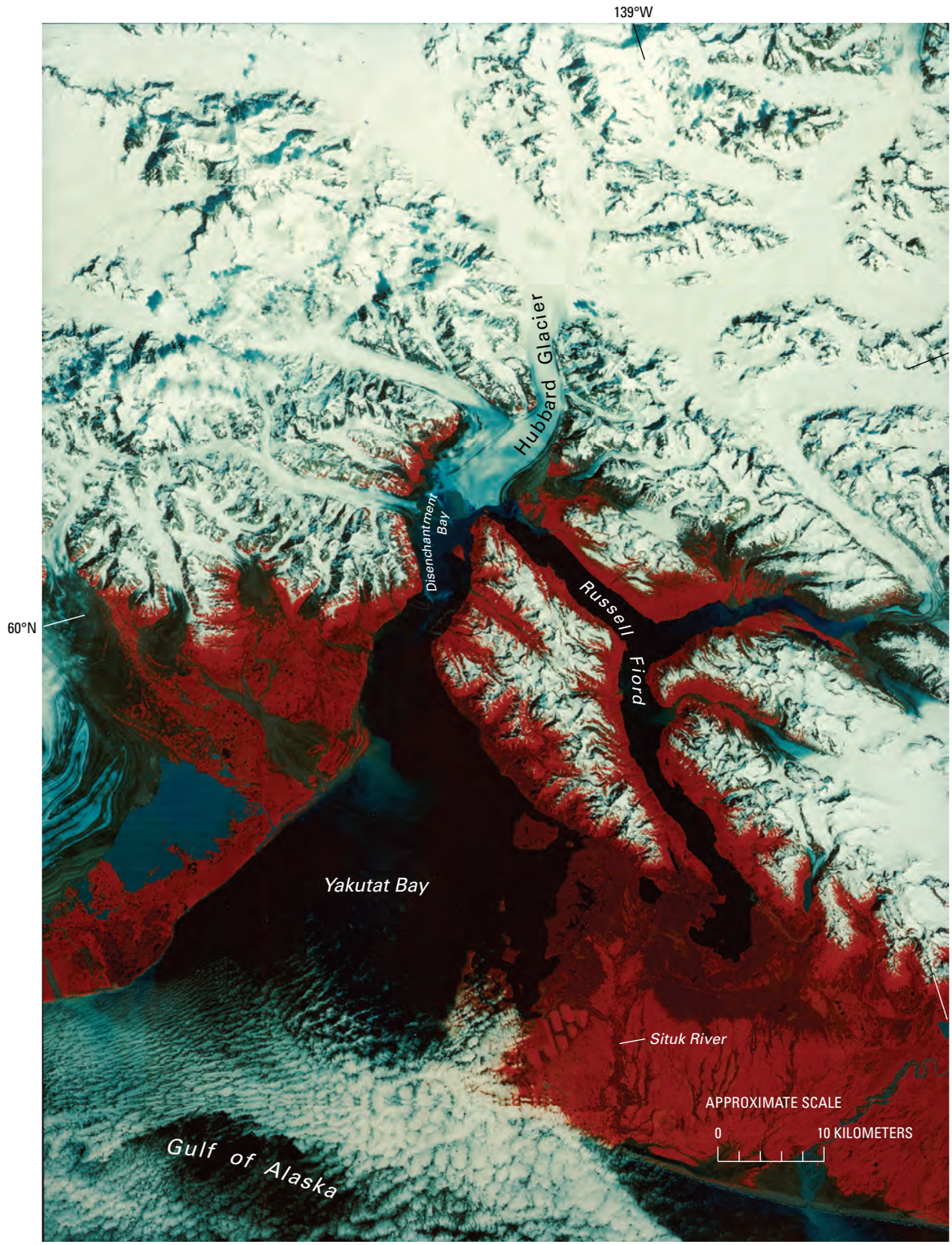

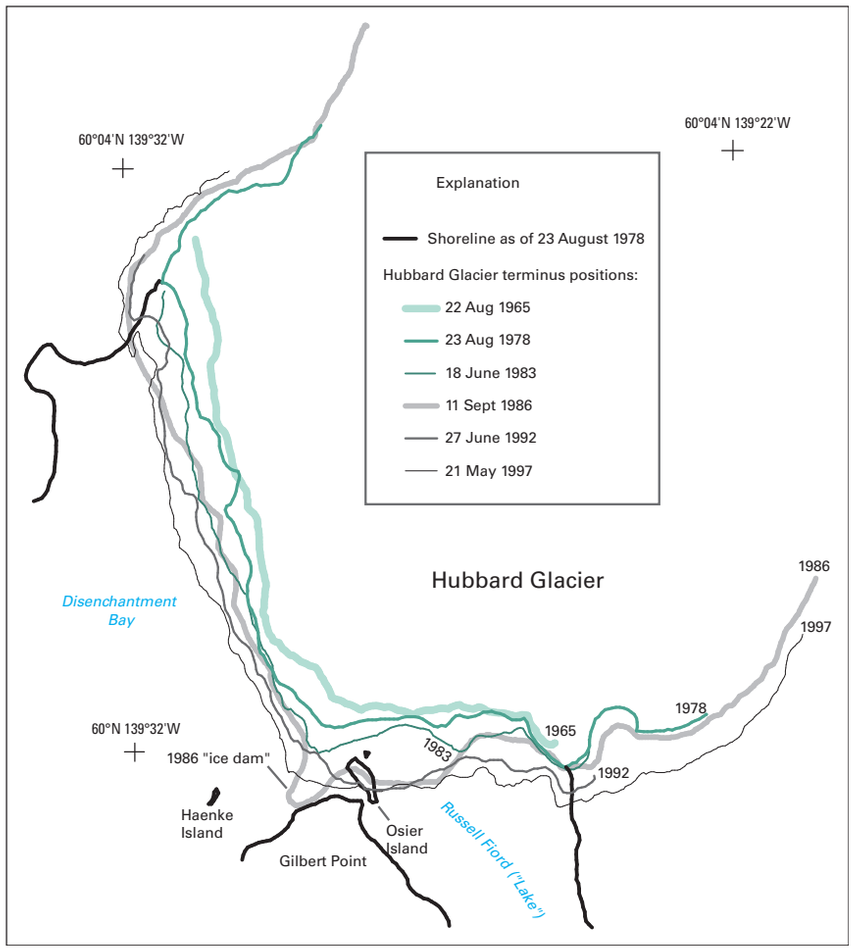

Figure 54.—*Advance of Hubbard Glacier terminus between 1965 and 1997. (Modified from Trabant and others, 2003.)*

Figure 55.—*29 August 1984 oblique aerial photograph of the terminus of the 112-km-long Hubbard Glacier, North America's largest tidewater glacier. This slowly advancing glacier closed the entrance to Russell Fiord in the spring of 1986 (see fig. 56) and again in 2002 (see fig. 157). On the date of this aerial photograph, the entrance to Russell Fiord (lower right) was about 500 m wide. Osier Island, in the entrance to the fjord, is about 500 m long. The Hubbard Glacier flows down the valley on the right from the St. Elias Mountains into Disenchantment Bay; the Valerie Glacier tributary merges into it from the left. Photograph No. 84–R1–082 by Robert M. Krimmel, U.S. Geological Survey.*

Under those conditions, *Russell Lake*, when full, drains via the Situk River to the south directly into the Gulf of Alaska. Moraines of Hubbard Glacier exist far beyond the position required for closure.

The general flow of Hubbard Glacier is regulated by its mass balance, which is largely controlled by the local climate and calving losses. Year-to-year

Figure 56.—*Oblique aerial photograph of the Hubbard Glacier ice dam on 12 September 1986, as it blocked the entrance to Russell Fiord (middle right center) at Gilbert Point (lower center). Osier Island is almost completely covered. A push moraine that formed as the glacier approached Gilbert Point reduced calving. The dam width is about 0.5 km. The ice dam, which formed in May 1986, created "Russell Lake." The ice dam failed because of calving and increased water pressure in Russell Fiord on 8 October 1986, releasing 5.3 km³ of water in less than 1 day. The maximum water discharge was estimated by Mayo (1988b) to be 104,500 m³ s⁻¹. Variegated Glacier (upper right) underwent a major surge in 1983. Photograph No. 86–R2–124 by Robert M. Krimmel, U.S. Geological Survey.*

changes of the AAR are an index to the climatically controlled accumulation and ablation components of mass balance. In many years since 1963, observations of the glacier near the end of the melt season have shown that the line separating the accumulation area from the ablation area (the equilibrium line) is normally at about 1,000 m in altitude. This equilibrium line altitude (ELA) gives Hubbard Glacier the extremely high AAR of 0.95, which demonstrates that the glacier's mass balance is very positive. As a result, Hubbard Glacier can easily sustain its calving and melt losses and increase its thickness while the terminus and its submarine terminal moraine advance farther into Disenchantment Bay. Furthermore, Hubbard Glacier is not currently sensitive to small climate changes. The equilibrium line lies on a steep, narrow part of the outlet glacier, where a 200-m increase in the ELA changes the AAR to 0.91 and a 200-m decrease in the ELA changes the AAR to 0.96. Changes in the ELA likely have been smaller than ±200 m for decades. For instance, the 1987–88 balance year resulted in a 50-m lowering of the ELA. This relatively small change was the response to winter precipitation that was about twice the 1951–80 normal amount, followed by a summer of near-normal temperatures, both of which suggest near-normal ablation (Trabant and others, 1990).

The accumulated ice mass must go somewhere. It is estimated that there is an ice flux of 6.8 $km^3\ a^{-1}$ through the cross section at the equilibrium line of Hubbard Glacier. This ice either is melted in the ablation zone (0.3 $km^3\ a^{-1}$),

increases the volume of the lower glacier by advance and increased thickness (0.05 $km^3 a^{-1}$), or calves (6.45 $km^3 a^{-1}$).

Surface-ice speeds of Hubbard Glacier measured in the ablation zone and near the equilibrium line are about 8 m d^{-1} near the terminus, 5 m d^{-1} in the central ablation area, and 12 m d^{-1} near the equilibrium line (Krimmel and Sikonia, 1986). Ice thickness also has been measured; the maximum thickness is about 700 m in the central ablation zone. The bed of the glacier is about 400 m below sea level at that location (Mayo, 1988a).

Hubbard Glacier also exhibits seasonal terminus changes. The glacier tends to advance in the winter and spring and retreat in the summer and fall (Krimmel and Trabant, 1992). These fluctuations may be caused by seasonal changes in calving rate or speed or by a combination of the two.

Alaska's tidewater glaciers (tables 2, 3; fig. 41), although large for North America, are relatively small in comparison with the large outlet glaciers from the ice sheets in the Antarctic and Greenland (Swithinbank, 1988; Weidick, 1995). Research on the Alaska glaciers is important, however, because the results of frequent and detailed observations on smaller glacier systems can be applied to the larger systems. Tidewater glaciers are unique in that the cycle of changing glacier size is indirectly related to climate (Post, 1975). The cycle for a specific tidewater glacier may be radically different from the cycle of land-terminating glaciers in the same region that is caused by climate change.

Surge-Type Glaciers

Most glaciers have relatively constant average annual flow rates. A small percentage exhibit substantial variations and major flow irregularities. When the average annual flow is relatively constant, variations that occur are generally predictable on a seasonal basis; longer period changes occur as the glacier responds to changes in mass balance. When the average annual flow is variable, some glaciers have dramatic annual velocity changes, often characterized by brief velocity increases of at least an order of magnitude. These glaciers are called surge-type glaciers. Surges involve large volumes of ice displacement and often are characterized by rapid advance of the glacier terminus. The first observed surge to be widely reported by the media in the United States occurred in 1937. The terminus of Black Rapids Glacier in the eastern Alaska Range advanced more than 5 km in less than a year (Time Magazine, 1937; Moffit, 1942). The terms "galloping glacier" and "runaway glacier" were widely used by the media to report this occurrence.

The first, and seminal treatise on surge-type glaciers was by Post (1960), followed by Meier and Post (1969) and Raymond (1987). Post (1969, p. 229) offered the following definition for a surge-type glacier: "one which periodically (15–100+ years) discharges an ice reservoir by means of a sudden, brief, large-scale ice displacement, which moves 10 to 100 or more times faster than the glacier's normal flow rate between surges." He continued "Glacier surges are not unique events which might result from exceptional conditions such as earthquakes, avalanches, or local increases in snow accumulation. These movements apparently are due to some remarkable instability which occurs at periodic intervals in certain glaciers." This comment about earthquakes and avalanches was in response to a theory of earthquake-induced glacier advance proposed by Tarr and Martin (1910) to explain changes that they observed in glaciers of the Yakutat Bay Region following the 1899 Yakutat Earthquake. Post (1965) concluded that the Great Alaska Earthquake of 1964 had not produced snow-and-ice avalanches or short-lived glacier advances in the Coast, St. Elias, Chugach, and Wrangell Mountains or in the

Alaska Range. Post (1965) coined the term "surge" because "advance" is frequently technically incorrect in that affected glaciers do not always advance beyond their former limits. The term "surge" is here used to describe sudden, large-scale, short-lived glacier movements that may or may not be associated with a terminal advance. Surge-type glaciers typically undergo alternating phases of short periods of active rapid flow, usually lasting from less than 1 to 3 years (surge), followed by much longer periods of slow flow lasting from 10 to 100 years (quiescence). The quiescent stage of a surge-type glacier may have seasonal velocity variations. Some glaciers, called "pulsing glaciers" (Mayo, 1978), exhibit frequent weak surges.

Surge-type glaciers have been observed in many parts of the world (for example, in the Pamirs, Tajikistan (Krimmel and others, 1976); and Svalbard (Liestøl, 1993, p. E127–E151), but one of the greatest concentrations of surge-type glaciers occurs in western North America, especially in the St. Elias, eastern Chugach, and eastern Wrangell Mountains, in parts of the Alaska Range, and in the Icefield Ranges adjacent to the U.S.- Canadian border (Post, 1969). In the regions that support surge-type glaciers, most glaciers do not surge. Post (1969) noted only 204 surge-type glaciers out of the several thousand western North American glaciers that he examined. About 75 percent of these surge-type glaciers were in Alaska. Clarke and others (1986) noted that only 6.4 percent (151 of 2,356) glaciers they examined in the St. Elias Mountains of Canada were of the surge type. However, more recent information has indicated that there are only 136 surge-type glaciers in the St. Elias Mountains of Canada (see also Clarke and Holdsworth, 2002b).

Most of the surge-type glaciers included in these studies were recognized from the air or from aerial photographs on the basis of their contorted medial moraines (Post, 1972) (fig. 57). Differential flow velocities and irregular flow conditions contort medial moraines and thus produce easily identifiable

Figure 57.—*Oblique aerial photograph of the Susitna Glacier, Alaska Range, showing contorted medial moraines indicative of a surging glacier. The glacier is approximately 3.5 km wide in the foreground. The 5 September 1966 photograph no. 667–40 is by Austin Post, U.S. Geological Survey.*

evidence of surging. Surge-type glaciers can also be recognized on Landsat images by their contorted medial moraines (see fig. 404).

Meier and Post (1969) identified 12 characteristics of surge-type glaciers:

> (1) All surge-type glaciers surge repeatedly, (2) Most surges are uniformly periodic, and the length of a surge cycle appears to be constant for a single glacier, (3) All surges take place in a relatively short period of time and are followed by a longer quiescent phase, (4) The time required for a complete surge cycle has no relation to the length, area, or speed of the glacier, (5) Total horizontal displacements of ice during the active phase are typically only a few kilometers but can be less than 1 km, (6) Most surges do not result in advance of the terminus, (7) An ice reservoir and an ice receiving area can be defined for all surges, (8) No abrupt bedrock sills, depressions, or ice dams are evident in most surging glaciers, (9) All sizes and kinds of glaciers surge, including glaciers in almost all climatic zones, (10) In western North America, surge-type glaciers occur only in certain restricted areas, (11) Western North American surge-type glaciers can be divided into three categories: type I, large to moderate length valley glaciers with very high speeds, large resulting displacements, and large-scale lowering of the ice reservoir; type II, large to moderate length valley glaciers with much smaller displacements and moderate lowering of the ice reservoir; and type III, small, steep glaciers with moderate lowering of the ice reservoir, (12) Whether there is a complete transition of glacier behavior from surge to normal is not known.

From the analysis of the characteristics of the 2,356 glaciers that they examined, Clarke and others (1986) determined that (1) long glaciers have a higher probability of being surge type than short glaciers do; (2) surge-type glaciers tend to have a higher overall elevation than normal glaciers do; and (3) surge-type glaciers have greater slopes in the accumulation zone and lesser slopes in the ablation zone. Later, Clarke (1991) concluded that surge-type glaciers tend to be longer and wider and to have lower overall slope than normal glaciers.

Water plays an important role in surging. Kamb and others (1985) found that high subglacial water pressures occur during rapid surge displacement. Variegated Glacier, a surge-type glacier, has been studied by many scientists (Balise and Raymond, 1985; Harrison and others, 1986; Humphrey and others, 1986; McMeeking and Johnson, 1986; Raymond and Malone, 1986; Raymond and others, 1987; Raymond and Harrison, 1987, 1988), who examined various aspects of basal-water pressure and storage of water. Kamb (1987) proposed that the mechanism for surge onset was based on the blockage of the linked-cavity network configuration of a glacier's basal water conduit system. Harrison and Post (2003) summarized the current state of knowledge about surge-type glaciers, with specific reference to Alaskan glaciers.

Sturm (1987) called the dry or water-filled depressions on glaciers that measure from a few meters to 100 m in diameter "potholes," Post and LaChapelle (1971, figs. 77, 78) called such depressions "lacunas." Sturm (1987) determined that fields of "potholes" usually are found on the surfaces of surge-type glaciers rather than on those of non-surge-type glaciers. After examining photographs of several thousand glaciers, Sturm determined that 21 of the 26 glaciers observed to have "potholes" were surge-type glaciers and that most "pothole" fields were found near the equilibrium line.

Glacier-Dammed Lakes and Glacier-Outburst Floods (Jökulhlaups)

Many Alaskan glaciers end in ice-marginal lakes formed by terminal or recessional moraines (fig. 58). Other glaciers form lakes by blocking or having distributaries that extend into adjacent valleys (fig. 59). (see also section on Columbia and Hubbard Tidewater Glaciers by Robert M. Krimmel in this volume.) Many Alaskan communities are located on rivers fed by glacial meltwater. Catastrophic flooding (jökulhlaups) caused by (1) drainage of ice-dammed lakes, (2) drainage of ice-marginal lakes, (3) release of water stored subglacially, englacially, or supraglacially, sometimes through surge-related processes, or (4) melting glaciers located around the summit craters of erupting volcanoes are a significant hazard. Annually, floods in Alaska cause many millions of dollars of damages (Lamke, 1991). Information about

Figure 58. *— 13 August 1982 AHAP false-color infrared vertical aerial photograph of the ice-marginal lake surrounding the terminus of Sheridan Glacier, Chugach Mountains, formed by the 20th century retreat of the glacier's terminus. The boundary between the darker red and lighter red vegetation surrounding the southern side of the lake marks the location of Sheridan Glacier's "Little Ice Age" end moraine. Note the icebergs in the ice-marginal lake. The debris-covered terminus of the Sherman Glacier is visible on the upper right of the photograph. Photograph No. L115F1516 from GeoData Center, Geophysical Institute, University of Alaska, Fairbanks, Alaska.*

the flooding history of Alaskan glaciers is presented in some of the sections that follow.

Stone (1963a) summarized the characteristics of 53 present and 7 former large ice-dammed lakes in an 1,285×160-km area of south-central and southeastern Alaska and adjacent Canada. His purpose was to call attention to "one of the world's greatest concentrations of lakes dammed by glacial [glacier] ice" (Stone, 1963a, p. 332). He defined these lakes as "impounded by glacial [glacier] ice touching the water, a minimum of ¼ to ½ mile [0.4–0.8 km] wide and ½ to 1½ mile [0.8–1.6 km] long, and with water supplied from one or two streams or glaciers in addition to the water from the damming glacier," (Stone, 1963a, p. 332). He noted that 11 of the 16 larger lakes have histories of regular or irregular emptying and that at least 6 ice-dammed lakes threaten transportation routes in Alaska. Three of the six lakes are located in Canada, but their floodwaters flow into the Pacific Ocean through Alaska via the Taku and Stikine Rivers. These six are (1) Lake George (Knik Glacier) (Stone, 1963a); (2) Hidden Creek Lake (Kennicott Glacier) (Anderson and

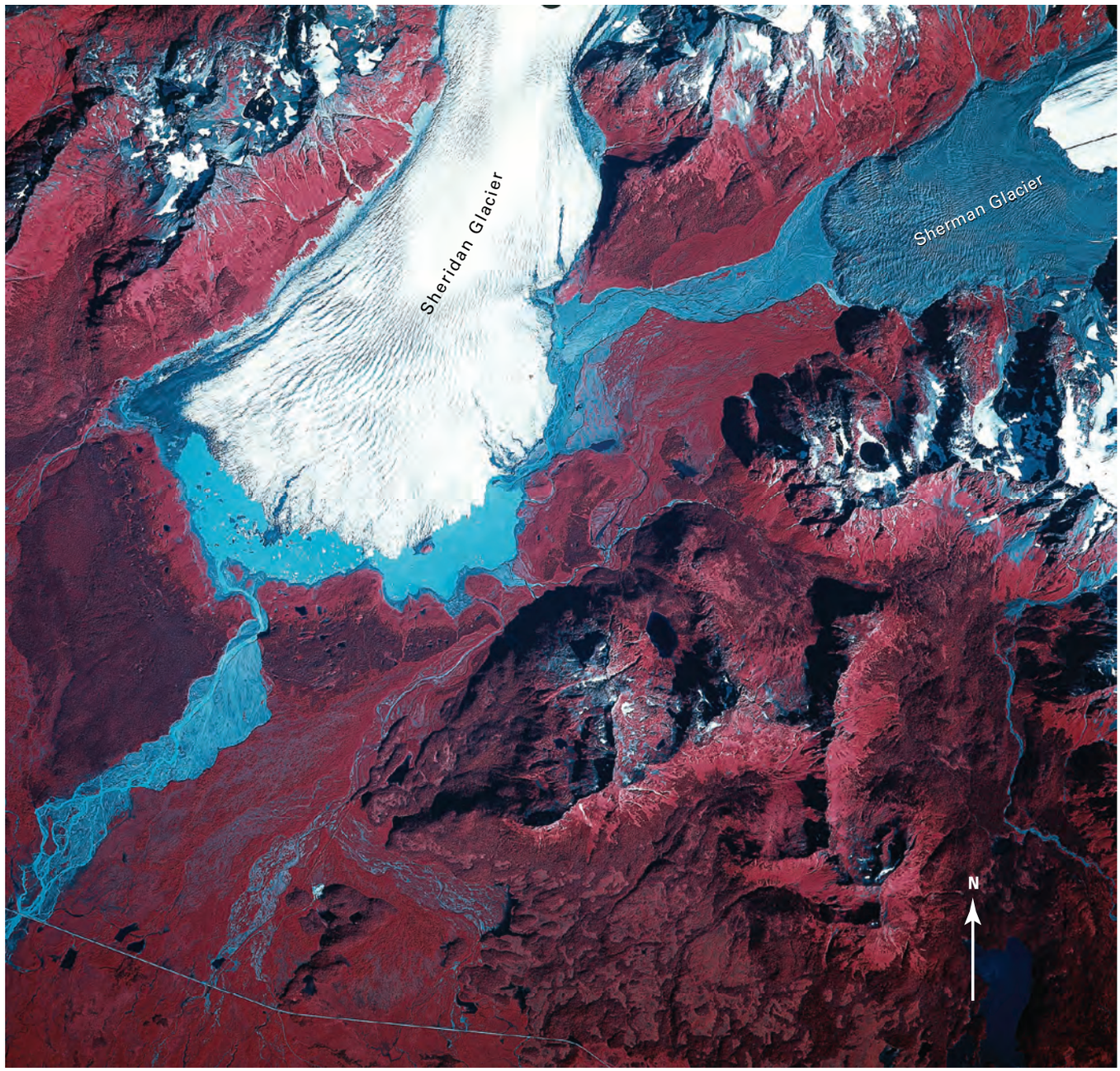

others, 2003); (3) Lower Skolai Lake (Nizina Glacier); (4) Tulsequah Lake (Tulsequah Glacier, Canada); (5) Flood Lake (Flood Glacier, Canada) (Ommanney, 2002a, fig. 21, p. J54); and (6) Great Lake (Great Glacier, Canada).

From an analysis of topographic maps and aerial photographs, Post and Mayo (1971) determined that there were 750 glacier-dammed lakes larger than 0.1 km^2 in south-central Alaska, southeastern Alaska, and adjacent Canada. They noted that additional glacier-dammed lakes are located in the Aleutian Islands, the Alaska Peninsula, Kodiak Island, and the Brooks Range. However, they did not include these lakes in their total. They presented maps showing the location of glacier-dammed lakes, glacier-clad volcanoes, and other areas subject to jökulhlaups and also gave information on the location and area of the lakes, the areas impacted, the type of hazards involved, individual histories of flooding for specific glacier-dammed lakes, and other available data about the glacier-dammed lakes.

Post and Mayo (1971) presented seven mechanisms through which glacier-dammed lakes form subglacial, englacial, or supraglacial channels that

Figure 59.—*20 July 1980 AHAP false-color infrared vertical aerial photograph of Kenibuna Lake, west of Shamrock Glacier, Chigmit Mountains, Aleutian Range, formed by damming of the Neacola River's valley. Chakachamna Lake, located to the east of Shamrock Glacier, is formed by the blockage of the eastern extension of this valley by Barrier Glacier. Recent retreat of Shamrock Glacier has resulted in the formation of an ice-marginal lake behind the glacier's "Little Ice Age" end moraine. Note the icebergs in the ice-marginal lake. Photograph No. L108F6633 is from GeoData Center, Geophysical Institute, University of Alaska, Fairbanks, Alaska.*

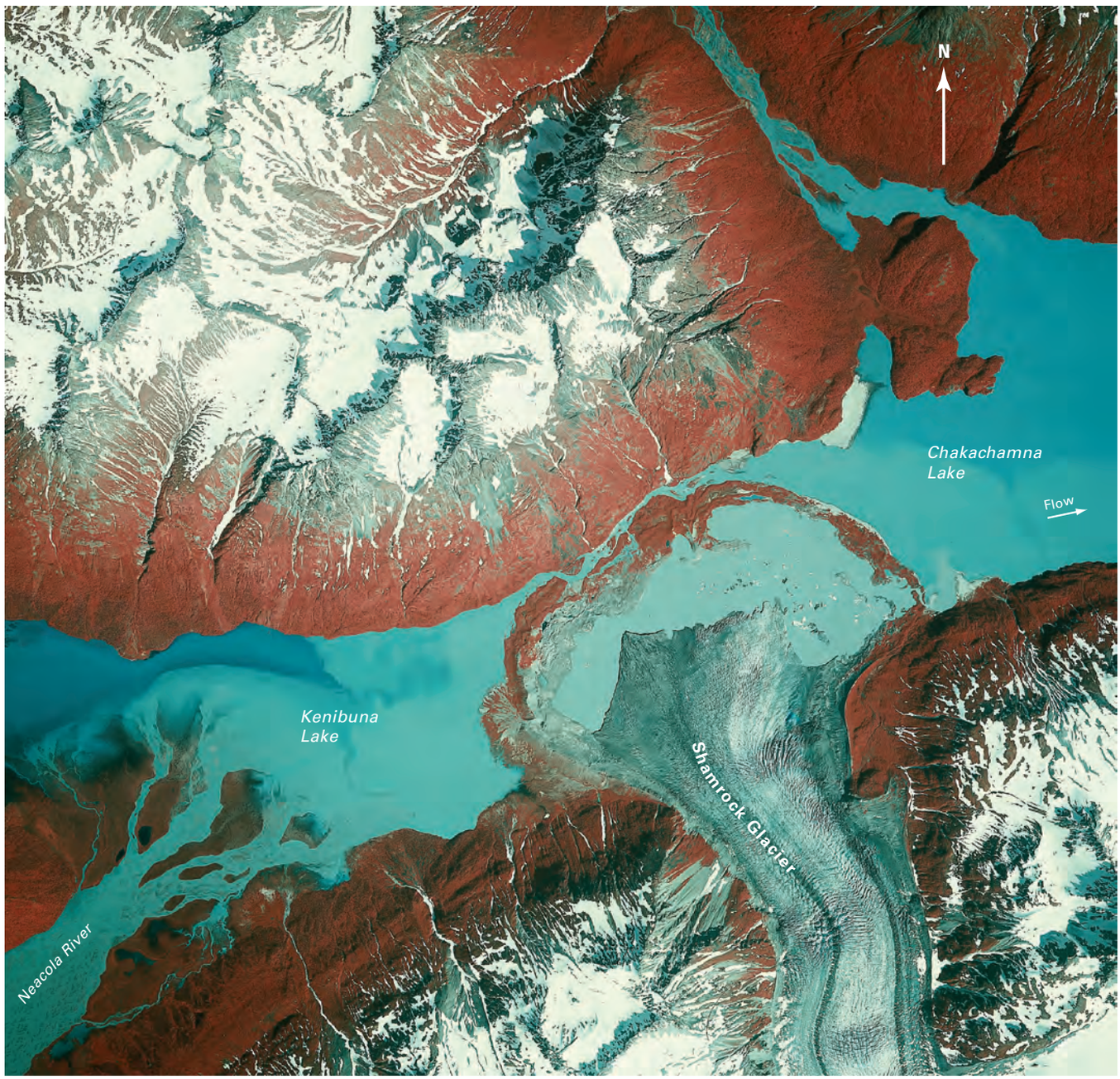

facilitate the release of water: (1) slow plastic yielding of the ice owing to hydrostatic pressure differences between the lake and the less dense ice (Glen, 1954); (2) raising of the ice dam by floating (Thorarinsson, 1939); (3) crack progression under combined shear stress owing to glacier flow and high hydrostatic pressure (Nichols and Miller, 1952); (4) drainage through small, preëxisting channels at the ice-rock interface or between crystals in the ice; (5) water overflowing the ice dam, generally along the margin (Liestøl, 1956); (6) subglacial melting by volcanic heat (Tryggvason, 1960); and (7) weakening of the dam by earthquakes (Tryggvason, 1960). All of these mechanisms are applicable to Alaskan glacier-dammed lakes. [Editors' note: Other related research on the physics of the failure of ice-dammed lakes and associated jökulhlaups include work on Lake Donjek (Donjek Glacier) (Collins and Clarke, 1977; Clarke and Mathews, 1981), work on ice-dammed lakes in Iceland (Björnsson, 1976, 1977), and theoretical work by Nye (1976) on Flood Lake in the Coast Mountains of British Columbia, Canada (Clarke and Waldron, 1984) (see also Clarke and Holdsworth, 2002a).]

Jökulhlaups at Bering Glacier

In the latter part of the 20th century (1981–84), jökulhlaups occurred from Berg Lakes on the western margin of the Steller Glacier in the Chugach Mountains. A second major outburst flood took place in 1986. The flooding of the river drainage west of the Bering Glacier was recorded on 12 September 1986 (fig. 60). In 1994, Bering Glacier in the Chugach Mountains experienced two jökulhlaups that significantly impacted local fauna and flora and modified the topography of adjacent land surfaces and the bathymetry of ice-marginal lakes. The glacier-outburst floods, both ice-margin, were of two different types: the catastrophic draining of an ice-dammed lake in May 1994 and the draining of surge-trapped water and sediment from an ice-margin outburst flood in July 1994 (Molnia, 1998).

The May 1994 flood resulted from the development of an approximately 500-m-long subglacial channel through and the subsequent failure of an ice dam at the northwestern margin of the Bering Glacier. The breaching of this tongue of ice lowered the surface level of 9×6-km Berg Lakes by more than 100 m (fig. 60*B*). An estimated 5.5 billion cubic meters of water escaped Berg Lakes and drained through Bering River during the ensuing 72-hour flood, completely inundating the Bering River valley from wall to wall. Because May is the time of moose calving and significant avian nesting activity—especially Dusky Canada Geese (*Branta canadensis occidentalis*) and Trumpeter Swans (*Olor buccinator*)—the outburst flood had a major impact on the local ecosystem. Post and Mayo (1971) previously stated that "lowering of the ice dam if continued will almost certainly lead to the release of immense floods in the near future. The Bering River flood plain and area surrounding Bering Lake are endangered by this increasingly critical situation" (cf. Post and Mayo, 1971, Sheet 3).

The July 1994 flood (fig. 61), which occurred on the southeastern margin of Bering Glacier approximately 45 km east of the May 1994 event, continued intermittently for more than a year. This flood event had estimated peak discharges in excess of 100,000 $m^3 s^{-1}$; it deposited about 0.3 km^3 of sediment and ice into the ice-margin lake system on the southeastern side of Bering Glacier. Buried ice-blocks continue to melt, initiating the formation of kettleholes and changing the surface morphology.

The 1994 floods were not unique. Bering Glacier has experienced similar flooding several times this century. Ice-dam failures at Berg Lakes have produced at least two similar floods in the last three decades. A 1967 aerial photograph taken by Post shows that a surge-terminating flood was occurring at about the same location that the 1994 eastern margin flood occurred. Bering Glacier floods have caused significant changes to the local environment.

Figure 60.—*Photographs of jökulhlaups at Bering Glacier.* **A**, *12 September 1986 oblique aerial photograph showing inundation of the Bering River and environs caused by a jökulhlaup from Berg Lakes. Photograph No. 86–R2–236 by Robert M. Krimmel, U.S. Geological Survey.* **B**, *Photograph looking across the basin of Berg Lakes, Bering Glacier, on 11 August 1998 showing the exposed lakebed produced by the catastrophic drainage of the lake in May 1994.The lake level was lowered by more than 100 m, and the jökulhlaup consisted of an estimated 5.5 billion m^3 of water. Photograph by Bruce F. Molnia, U.S. Geological Survey.*

Jaeger and Nittrouer (1999a) examined Gulf of Alaska marine sediments looking for evidence of jökulhlaups from Bering Glacier. In a 250-cm-long core collected at the head of Bering Trough, they identified six laminated, high-porosity beds from 1994, 1953(±4), 1938(±6), 1917(±8), 1899(±10), and 1874(±13). They correlated five of these beds with 20th century floods associated with surges reported by Molnia and Post (1995) that occurred in 1994, 1957–60, 1938–40, 1920, and 1900. No bed was identified that correlated with an observed jökulhlaup in 1967 that marked the end of the 1965–67 surge. Their 1874 bed probably correlates with a surge that has no remaining surficial evidence.

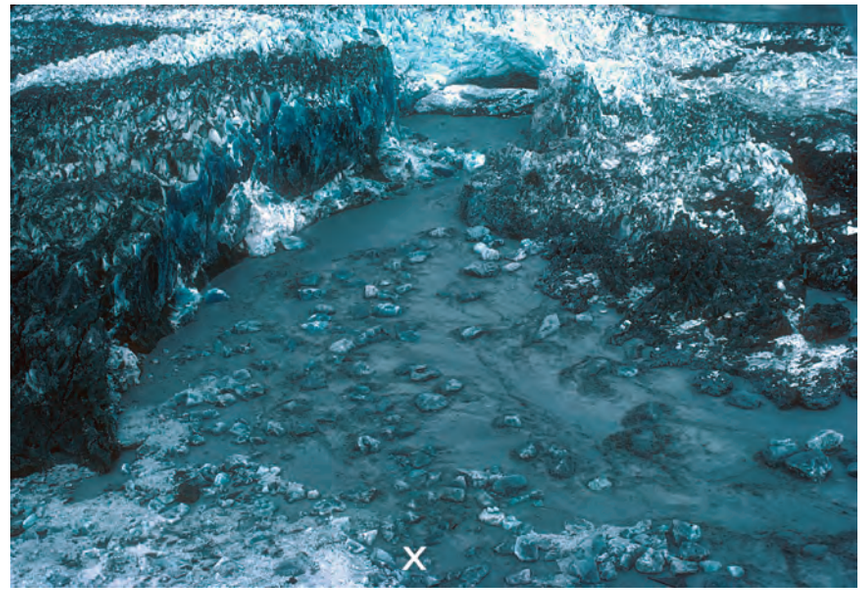

Figure 61.—*Oblique color aerial photograph of the channel cut through the eastern terminus of the Bering Glacier by a jökulhlaup that initially discharged at the face of the glacier (the point marked by the "X" on the photograph). At the time this 29 July 1994 photograph was taken, less than 24 hours after the start of the jökulhlaup, the point of discharge had retreated nearly 0.8 km. Photograph by Bruce F. Molnia, U.S. Geological Survey.*

Debris-Covered Glaciers

Hundreds—probably thousands(?)—of Alaskan glaciers are partially, if not completely, covered by supraglacial sediment ranging in thickness from a few millimeters to many meters. Glaciers with large concentrations of supraglacial sediment are called "debris-covered glaciers." Debris on glaciers is the result of a variety of mass-wasting, ice-transport, hydrologic, and eolian (including tephra) sediment-transport processes. The debris often has a significant influence on the rate of ablation of the ice located underneath, and most debris-covered glaciers have their greatest amount of debris, in area and (or) in thickness, in their ablation areas. However, some glaciers, especially those where the debris cover is the result of mass-wasting processes, may have their debris cover on either the accumulation areas or the ablation areas of the glacier (or both). On some glaciers, the thickness of supraglacial debris can exceed 15 m. Mature forests, often with trees more than 50 cm in breast-height diameter (BHD), grow on the debris-covered termini of more than a dozen glaciers in south-central Alaska, including Bering, Malaspina, Fairweather, and Yakataga Glaciers.

The origin of glacier debris varies from glacier to glacier and from geographic region to geographic region. With respect to mass-wasting processes, supraglacial debris on Alaskan glaciers can result from avalanching of snow, ice, and rock from adjacent valley walls; from rock avalanches caused by earthquakes, high-precipitation rainfall events, and other triggering processes; from solifluction from adjacent surfaces; and from frost wedging. The March 1964 *Good Friday* earthquake caused more than 100 rock avalanches onto glaciers in the Chugach and St. Elias Mountains (Post, 1967a) (see also figs. 58, 228, 229). Similarly, the 2 November 2002 M7.9 earthquake along the Denali Fault generated several large rock avalanches on a number of glaciers in the Alaska Range (see fig. 394). Typically, debris formed by mass-wasting processes is distinguishable by its angular character. Often, however, supraglacial debris transported by mass-wasting processes is reworked by glaciological and fluvioglacial processes.

With respect to ice-transport processes, most debris on Alaskan glaciers results from concentration in the ablation area of sediment transported downglacier as englacial debris or as medial and lateral moraines. Debris produced in this fashion is also often reworked by aeolian and fluvial processes.

With respect to sedimentological processes, debris on Alaskan glaciers can also result from transport of sediment onto the glacier's surface by glacier-outburst floods (jökulhlaups) resulting from the failure of ice-dammed lakes in tributary valleys and from upglacier, ice-marginal lakes; from subglacial geothermal and (or) volcanic activity; from eolian transport of adjacent sand, silt, and clay, especially from the outwash plain; from the fall of volcanic tephra; and from lahar-type deposits originating from the summits or along drainage systems of glacier-covered volcanoes.

At many glaciers, ablation moraine produced by a combination of processes is reworked by meltwater and results in both winnowing and stratification of the deposits. Following initial deposition, much of a glacier's supraglacial debris is subject to secondary reworking.

Many Alaskan glaciers include a stagnant-ice zone characterized by thick accumulations of surface debris. One of the first of these glaciers to be studied in detail was the Martin River Glacier, located in the Chugach Mountains east of the Copper River. There, the evolution of a sequence of thermokarst landforms, including water-filled, sinkhole-like lakes, was documented by Reid and Clayton (1963) and Clayton (1964). Many glaciers with thermokarst lakes are the sites of high-discharge jökulhlaups. The evolution and growth of these lakes during the melting of the ice beneath the sediment are the focus of much recent research (Nakawo and others, 2000).

Stagnant, debris-covered ice goes through a geomorphological process that results in the final melting of buried ice, generally during a period of several decades to centuries, and the formation of a hummocky topography frequently referred to as "kame-and-kettle" topography. During the ablation process, local differences in the thickness of the insulating debris cover, combined with redistribution of sediment, result in differential ablation of the underlying ice and the formation of thermokarst pits, many of which support supraglacial lakes and ponds. As these lakes and ponds evolve, they frequently drain and cause flooding downstream from the glacier's terminus.

Richardson and Reynolds (2000) studied processes leading to ice-cored moraine degradation for three natural dams in Perú and Nepal. They noted that potentially hazardous lakes form on the snouts of debris-covered glaciers and that this occurrence may separate a stagnant-ice body from the upper reaches of the glacier to form an ice-cored, end-moraine complex. They described a process that ultimately results in a jökulhlaup. Degradation through ablation beneath the debris cover by localized thermokarst development and by associated loss of ice mass leads to lake expansion, typically along glacier crevasses and other internal glacier structures. Once exposed, the ice undergoes accelerated wastage through the combined effects of solar radiation and mechanical failure caused by the rheological response of the ice to deepening ice depressions. Continuing degradation reduces the lake "freeboard" and weakens the moraine dam, thereby setting the stage for catastrophic failure of the dam.

Debris-covered ice melts at a slower rate than bare glacier ice under similar conditions. If the protective debris cover is sufficiently thick, the ablation rate approaches zero, as it does at the terminus region of Sherman Glacier (see figs. 58, 229). On the other hand, a thin debris cover may act as a heat sink and cause the rate of the melting of the ice to increase immediately below. Although no studies of Alaskan glaciers were found comparing ablation rates for adjacent bare and debris-covered ice, investigations have been conducted on temperate glaciers at several locations. [Editors' note: According to Mark F. Meier (written commun., 2004), Driedger's (1981) research on the effect of tephra fall on the melting of ice and snow on Mount St. Helens, Wash., concluded that the "breakeven point" between accelerated melting and insulation occurred at a thickness of 2.5 cm.]

Kayastha and others (2000) studied the ablation of bare and debris-covered ice on Khumbu Glacier, Nepal, from 21 May to 1 June 1999 to determine

how the sediment cover affected the relationship between the positive degree-day factor and the ablation rate. They found that, with a debris cover ranging in thickness from 0 to 5 cm, ice ablation was at its maximum with a debris cover of 0.3 cm and that debris thicker than 5 cm retarded ablation. Ice ablation from net solar radiation was measured at several depths on the glacier. On a bare ice surface, ablation was 16.9 mm d^{-1}. Under 10- and 40-cm-thick debris layers, ablation was 11.1 and 5.3 mm d^{-1}, respectively. Similarly, Takeuchi and others (2000) measured ablation and heat balance in debris-covered and debris-free areas of the ablation zone at Khumbu Glacier during the same period of time. They found that ablation rates on the debris-free ice ranged from 1.4 to 4.7 cm d^{-1} and were inversely correlated with the albedo. Melting of debris-covered ice decreased sharply with increasing thickness. Debris with a thickness of 10 cm slowed melting to about 40 percent of the rate of bare ice at the same low albedo. The primary cause of melt reduction was the insulating effect of the debris cover. Interestingly, they also found that the heat stored in the debris layer during daytime was released to the atmosphere during nighttime and warmed the air rather than being conducted downward to melt ice.

As part of ongoing annual mass balance measurements on Lyman Glacier and Columbia Glacier, North Cascades, Wash., Pelto (2000) measured ablation of ice on adjacent clean and debris-covered sections of each glacier. For Columbia Glacier, between 1986 and 1998, the annual ice ablation was 3.3 m water equivalent for clean glacier ice and 2.3 m water equivalent for debris-covered areas. For Lyman Glacier from 1986 to 1999, the average annual ablation on the clean glacier ice was 3.4 m; under the debris cover, average annual ablation was 2.6 m water equivalent.

Finally, debris-covered glaciers pose a problem for monitoring glacier change by means of remote sensing techniques, especially those using medium- to low- resolution multispectral instruments. A debris-covered surface of a glacier has a spectral reflectance similar to that of adjacent bedrock or sediment bodies. Often, the glacier's debris cover and the adjacent ice-marginal sediment are derived from the same bedrock and therefore have the same composition. Given the lower spatial resolution of large picture elements (pixels), the ability to discriminate between supraglacial, moraine, and outwash deposits on the basis of morphological characteristics is also greatly diminished.